IEEE Access
Multidisciplinary | Rapid Review | Open Access Journal

Received July 15, 2021, accepted August 7, 2021, date of publication August 13, 2021, date of current version August 24, 2021.

Digital Object Identifier 10.1109/ACCESS.2021.3104617

Grid Forming Inverter Modeling, Control, and Applications

DAYAN B. RATHNAYAKE[1], (Student Member, IEEE), MILAD AKRAMI[2], CHITARANJAN PHURAILATPAM[3], (Graduate Student Member, IEEE), SI PHU ME[1], (Graduate Student Member, IEEE), SAJJAD HADAVI[1], (Student Member, IEEE), GAMINI JAYASINGHE[1], (Senior Member, IEEE), SASAN ZABIHI[1,4], (Senior Member, IEEE), AND BEHROOZ BAHRANI[1], (Senior Member, IEEE)

[1]Department of Electrical and Computer Systems Engineering, Monash University, Clayton, VIC 3800, Australia
[2]Doctoral School of Mathematics, Information Sciences, and Engineering, University of Strasbourg, 67081 Strasbourg, France
[3]IITB-Monash Research Academy, IIT Bombay, Mumbai 400076, India
[4]Hitachi ABB Power Grids, Fortitude Valley, QLD 4006, Australia

Corresponding author: Dayan B. Rathnayake (dayan.rathnayake@monash.edu)

This work was supported by the Australian Renewable Energy Agency (ARENA) through the Advancing Renewable Program under Grant 2020/ARP007.

ABSTRACT This paper surveys current literature on modeling methods, control techniques, protection schemes, applications, and real-world implementations pertaining to grid forming inverters (GFMIs). Electric power systems are increasingly being augmented with inverter-based resources (IBRs). While having a growing share of IBRs, conventional synchronous generator-based voltage and frequency control mechanisms are still prevalent in the power industry. Therefore, IBRs are experiencing a growing demand for mimicking the behavior of synchronous generators, which is not possible with conventional grid following inverters (GFLIs). As a solution, the concept of GFMIs is currently emerging, which is drawing increased attention from academia and the industry. This paper presents a comprehensive review of GFMIs covering recent advancements in control technologies, fault ride-through capabilities, stability enhancement measures, and practical implementations. Moreover, the challenges in adding GFMIs into existing power systems, including a seamless transition from grid-connected mode to the standalone mode and vice versa, are also discussed in detail. Recently commissioned projects in Australia, the UK, and the US are taken as examples to highlight the trend in the power industry in adding GFMIs to address issues related to weak grid scenarios. Research directions in terms of voltage control, frequency control, system strength improvement, and regulatory framework are also discussed. This paper serves as a resource for researchers and power system engineers exploring solutions to the emerging problems with high penetration of IBRs, focusing on GFMIs.

INDEX TERMS Current control, fault ride-through, grid forming inverters, power synchronization control, small-signal and transient stability, virtual inertia.

I. INTRODUCTION

Conventional AC power systems are dominated by synchronous generators, where the primary control objectives of voltage and frequency regulation are achieved through exciter control and governor control, respectively. Low output impedance, together with the automatic voltage regulation action, make synchronous generators near-ideal voltage sources. Moreover, the inertia of the prime-mover and rotor helps keep frequency within the operating limits during disturbances such as load changes and faults. This ideal voltage source behavior and high inertia are the essential features for maintaining a stable power grid. In addition, the extensive fault current handling capability of the synchronous generators, typically up to six times the rated current, is an essential feature in clearing faults.

With the growing demand for renewable energy technologies, mainly wind and solar, inverter-based resources (IBRs) are becoming an inevitable part of AC power systems. Due to the intermittent nature of these sources, IBRs often tend

The associate editor coordinating the review of this manuscript and approving it for publication was Guangya Yang.

This work is licensed under a Creative Commons Attribution 4.0 License. For more information, see https://creativecommons.org/licenses/by/4.0/

to extract the maximum available power at any time and feed the extracted power into the grid. The inverters used in IBRs are generally designed to follow the grid voltages and inject current into the existing voltage. Therefore, they are known as grid following inverters (GFLIs). The common technique used to synchronize with the grid voltage is the use of a phase-locked loop (PLL). This particular grid following behavior resembles a current source. Almost all of the currently installed IBRs fall into this category, and thus, voltage source behavior is not intrinsically present in IBRs. Moreover, IBRs are not designed with sufficiently large energy storage to emulate inertial response. The over-current ratings of the power electronic switching devices used in inverters are also very low compared to synchronous generators. Therefore, IBRs are considered as non-synchronous generation sources. The major challenge with the increased penetration of non-synchronous generation sources in power systems is the voltage and frequency regulation [1].

Microgrids, which can operate in the grid-connected mode as well as in the islanded mode, emerged as a platform for integrating IBRs [2]. In the grid-connected mode, voltage and frequency are regulated by the grid, and thus, IBRs simply operate as grid following inverters. In the islanded mode, one of the inverters, or a couple of them, should function as voltage and/or frequency regulator(s) to form a local power grid. The concept of grid forming inverters (GFMIs) originated from this particular need. Furthermore, the need for emulating the features of the synchronous generators emerged as the concept of microgrids evolved. Thus, energy storage elements and control solutions, including virtual synchronous generator operation, are also developed as enhancements for GFMIs [3], [4].

Even though GFMIs were originally developed for the use in islanded microgrids, the concept can be adapted for applications in large power systems, especially in integrating wind and solar farms. Since wind and solar farms are often located in remote sites, the line impedance tends to be high. Such sections of the grid are termed as weaker parts of the grid. Voltage regulation at the point of common coupling (PCC), through conventional solutions, becomes challenging in weak grids. GFMIs provide a promising solution to this issue by strengthening the grid.

GFMI technology is still in its infancy. Therefore, modeling techniques, control methodologies, challenges, and various applications of GFMIs are relatively unknown. To address this gap in knowledge, several papers have reviewed the pertinent literature on different aspect of GFMIs. In [5], the authors have investigated various types of virtual synchronous generator (VSG) control methods, their challenges, potential future work, and their use in grid frequency control. However, other types of GFMIs are not covered in [5]. Furthermore, the mentioned challenges include computing techniques, modeling and analysis tools, robustness issues, and grid coordination, and they are all exclusive to VSG-based controllers.

A review regarding virtual inertia and related issues are discussed in [6], and various methods and their typologies, including synchronous generator model-based, swing equation-based, frequency-power response-based, and droop-based control methods are discussed. Additionally, Reference [6] addresses issues related to virtual inertia modeling, estimation, and marketing.

A comprehensive review of different types of virtual synchronous machine (VSM) control methods for wind turbines (WTs) is done in [7]. This paper discusses several challenges associated with the application of VSM-based control methods in WTs, including operating in weak grids, fault-ride through (FRT) capability, and frequency control. The paper, however, does not cover other types of GFMIs. Also, VSM control methods are not discussed for other types of renewable energy sources. Several grid forming control methods are reviewed and discussed in [8]. The paper, however, failed to address their main challenges and various applications.

A review and classification of several grid forming control algorithms is conducted in [9] and [10]. There are also discussions regarding the challenges of GFMIs, such as synchronization stability, FRT capability, and current limitation methods, as well as transitions between grid-connected and standalone modes. However, the applications of GFMIs are not discussed in the article. In addition, some grid forming control methods are not presented in the paper.

A review on requirements and solutions for issues in future low-inertia power systems is done in [11]. The issues related to reduced inertia and various technologies and control techniques that can offset the inertia shortfall are discussed. To this end, GFMI technology is recognized as a prominent driver towards future renewable energy rich power systems. Therefore, some of the well-known synchronous machine-based control techniques are discussed. Further, the applications of GFMIs in WTs and photovoltaic systems are covered. However, many of the GFMI control techniques that are in the literature are missing. Further, some of the important aspects pertaining to GFMIs such as modeling methods, stability analysis, and protection schemes are not covered.

The above discussion illustrates how current review papers have failed to address some key aspects of GFMI research. This includes evaluation of all grid forming control methods, analysis of the main challenges of GFMIs, and in parallel, a study of their applications. A comparison between the already available review papers is shown in Table 1. As the technology is relatively new, a comprehensive survey of GFMIs, covering modeling, control, stability analysis, fault handling, and applications, is not available in the current literature. Therefore, this paper aims to fill this gap with recent developments, applications, and future trends of GFMIs. This paper serves as a useful resource for researchers starting their studies on GFMIs and power system engineers exploring solutions to the emerging problems with high penetration of IBRs.

The main contributions of this paper are summarized as follows:

TABLE 1. Comparison between existing review papers.

Paper	Modeling methods	Control techniques	Stability analysis	Protection schemes	Applications of GFMIs	Real-world implementations
[5]	✗	✓[1]	✗	✗	✓[2]	✗
[6]	✗	✓[3]	✗	✗	✗	✗
[7]	✗	✓[4]	✗	✓	✓[5]	✓[6]
[8]	✓	✓	✗	✗	✗	✗
[9]	✗	✓[7]	✗	✓	✗	✗
[10]	✓	✓[8]	✓	✓	✗	✗
[11]	✗	✓[9]	✗	✗	✓	✗
This paper	✓	✓	✓	✓	✓	✓

1, 2- The mentioned control methods and applications are all exclusive to VSG-based controllers.
3- Only the synchronous machine-based control methods are reviewed.
4- Only some of the synchronous machine-based control methods are discussed.
5- Only focuses on the use of VSM control methods for WTs.
6- A few implementations related to WTs are discussed.
7- Only a few synchronous machine-based control methods are discussed.
8- Only a few synchronous machine-based control methods and virtual oscillator control are discussed.
9- Only some of the machine-based control methods are reviewed.

- This paper provides a comprehensive review of the topic after reviewing over 160 papers and considering various control methods for GFMIs including a detailed comparison of the GFMI control methodologies.
- Various applications of GFMIs in renewable energy sources, weak grids, high-voltage direct current HVDC) converters, and black-start operation are discussed.
- Key challenges and issues with GFMIs, such as transient and small-signal stability, FRT capability, overcurrent protection, and the transition between grid-connected and standalone modes are outlined in detail.
- The paper describes current GFMI projects around the world that are not addressed in the previous review papers.

The paper is organized as follows. Section II provides a comparison of GFLIs and GFMIs, highlighting their salient features. Section III presents a comprehensive discussion on modeling and control technologies related to GFMIs. A detailed discussion on GFMI challenges is presented in Section IV. The applications of GFMIs are discussed in Section V with a list of recent implementations. Future trends and research directions of GFMIs are discussed in Section VI.

II. COMPARISON OF GRID FOLLOWING AND GRID FORMING INVERTERS

The primary objective of supplying active and reactive power to the grid is common for all IBRs. However, depending on the interaction with the grid, controller implementation and response to the changes in the grid, they can be classified into two main groups, namely: GFLIs and GFMIs, as shown in Fig. 1 (a) [12]. More information, including further subdivisions of the two categories, are given in the following subsections.

A. GRID INTERACTION CAPABILITIES OF GFLIs AND GFMIs

As mentioned in the introduction, applications of GFLIs are primarily focused on active power injection into the grid with maximum power point tracking (MPPT). Therefore, the reactive power supply is minimum and often close to zero. Such inverters are known as grid-feeding inverters (GFDIs). From a revenue point of view, it is more attractive to run IBRs as GFDIs. Nevertheless, voltage and frequency regulation become challenging as the number of GFDIs increases. Therefore, grid operators/regulators have imposed strict requirements, especially on large-scale IBRs (typically above 5 MW), to support the grid by supplying reactive power and varying active power in response to the changes in the grid. An example Q response requirement is illustrated in Fig. 1 (b), where the reactive power response kicks in to support the grid voltage when there is a deviation [12]. When the grid voltage decreases, the IBR should supply positive reactive power at a predefined droop setting. Similarly, when the voltage increases, negative reactive power should be supplied by the IBR, as shown in Fig. 1 (b). IBRs that operate in the grid supporting mode are known as grid-supporting inverters (GSIs). Almost all the large-scale IBRs work as GSIs, and small-scale IBRs, typically below 5 MW, operate as GFDIs.

The fundamental difference in grid interaction of GFMIs come from the way active and reactive power delivery to the grid is controlled. As mentioned above, the primary objective of GFLIs is to inject active power to the grid, and supporting the grid is the secondary objective. In contrast, in GFMIs, the primary objective is regulating the voltage and frequency of the grid. Therefore, active and reactive power references are continuously varied in GFMIs to achieve this objective.

B. CONTROL IMPLEMENTATION

From the control point of view, the behavior of a GFLI can be approximated to a controlled current source with a high impedance in parallel, as shown in Fig. 2 (a). A GFLI measures the voltage at the PCC (v_{PCC}) and derives the phase angle of the v_{PCC} via a PLL. Then, the terminal voltage is varied such that the desired direct- and quadrature- ($d-q$) line currents are achieved. The active and reactive power

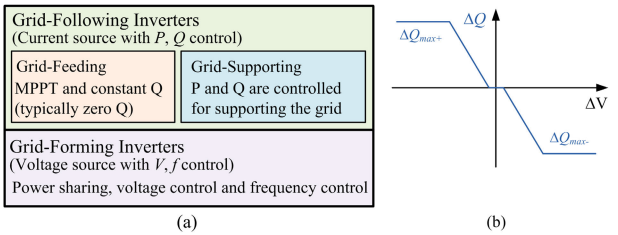

FIGURE 1. (a) Classification of grid-connected inverters and (b) reactive power control for supporting the grid.

support from a GFLI is achieved by controlling the injected d and q currents, respectively. In contrast to a GFLI, a GFMI can be approximated to a voltage source with a low series impedance, as shown in Fig. 2 (b). Contrary to GFLIs, GFMIs do not measure the v_{PCC} for synchronization purposes and rather form the v_{PCC} to regulate their power output. Another major difference between the GFLI and GFMI control is that a GFMI can operate/supply the local loads in the absence of grid connection by establishing its own reference voltage and frequency [8], [9], [12]–[14]. This also leads to the difference in synchronization mechanism. A GFLI requires a dedicated synchronizing unit to remain or operate in synchronism with the grid and push a specific amount of active and reactive power to the grid. However, in GFMIs, synchronization at the beginning of the operation can be achieved in a similar manner to a synchronous machine, and a dedicated synchronization mechanism is not required during the normal operation.

C. PERFORMANCE COMPARISON

In a steady-state operating condition, depending on the control topology, power set-points and grid conditions, both GFLIs and GFMIs can inject active and reactive power to the grid. However, one of the main differences in performance between GFLIs and GFMIs lies in the reaction of each of these inverters to a grid disturbance in weak grids. Active and reactive power support during a disturbance, which is also known as virtual or emulated inertia support, can be implemented in both GFLIs and GFMIs depending on the source type. In the case of a GFLI, the disturbance is measured through voltage and current measurements, and appropriate control actions are taken for grid support functionality. Thus, the active or reactive power response of a GFLI is associated with some form of measurement and control delay. However, in the case of a GFMI, the power transfer equation at the beginning of the disturbance is given as

$$P = \frac{V_s V_r}{X} \sin \Delta\delta, \tag{1}$$

where V_s is the sending end or the internal voltage, V_r is the receiving end or the grid voltage, X is the coupling impedance, and $\Delta\delta$ is the phase angle difference between the internal voltage and the grid voltage. As the internal voltage phasor of the GFMI is not affected at the beginning of the disturbance, an instantaneous response of power can

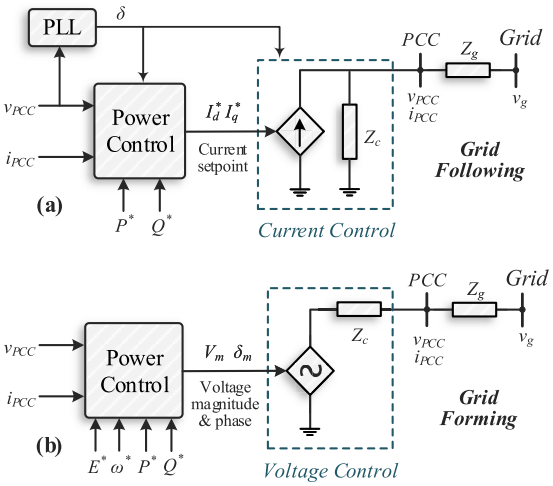

FIGURE 2. Comparison of control and approximation of (a) GFLI and (b) GFMI [9], [15].

be achieved depending on how fast the grid angle changes. Even though the reaction of a GFMI is much faster compared to its GFLI counterpart, concerns on current limitations and stability with rapid responses need to be addressed.

Another difference in the performance between GFMI and GFLI control is the small-signal stability behavior under weak grid conditions. With GFLIs relying on grid voltage and angle measurements to remain synchronized to the grid, the stability margin can be greatly reduced with sudden changes in the measured grid signals. This problem is greatly reduced in GFMIs with the possibility of self-synchronization and the absence of dependency on grid signals for synchronous operation.

Detailed discussions on the control methodology, performance, and limitations of the GFMIs are provided in the following sections.

D. ENERGY STORAGE AND OVER-SIZING

As mentioned in the introduction, GFMIs are expected to perform as synchronous generators, and thus, it is essential to emulate the important features of synchronous generators, such as the ability to supply constant/committed power to the grid, inertial response, and fault current behavior as much as possible. Some form of energy storage is required to maintain committed power delivery, irrespective of the changes in the wind or solar power input. Similarly, the inertial response requires energy storage, at least for the duration of the required response. Therefore, the need for energy storage is another major difference between GFLIs and GFMIs. Alternative approaches that have been proposed to manage the energy storage requirements in GFMIs attached to wind farms are discussed in Section VI. Meeting the fault current behavior of the synchronous generators is challenging in GFMIs with the current limitations in switching devices. Therefore, GFMIs have to be oversized, which makes them expensive and commercially less attractive.

III. GRID FORMING INVERTER MODELING AND CONTROL METHODS

A. GFMI MODELING METHODS

The power stage of a typical GFMI is shown in Fig. 3. The active and reactive power (P, Q) outputs from the inverter can be expressed as

$$P = \frac{3}{R_g^2 + X_g^2}(R_g V_c^2 - R_g V_c V_g \cos\delta + X_g V_c V_g \sin\delta) \quad (2)$$

$$Q = \frac{3}{R_g^2 + X_g^2}(X_g V_c^2 - X_g V_c V_g \cos\delta - R_g V_c V_g \sin\delta), \quad (3)$$

where R_g, X_g, V_c, V_g, and δ are the grid resistance, grid reactance, inverter-side RMS voltage, grid-side RMS voltage, and phase angle difference between the grid and the inverter, respectively. In [16], a small-signal model of the plant is presented by linearizing (2) and (3) around an operating point. This model is valid only for high inertial systems where the power system is dominated by synchronous machines, as it neglects the dynamics of the network elements. Therefore, a dynamic phasors-based model is proposed in [17] to analyze the small-signal stability of droop controlled inverters. This modeling approach captures the fast dynamics of the network components. Hence, it is particularly suitable for inverter-dominated power systems.

The modeling of GFMIs in the sequence domain, with applications in power system studies such as load flow and fault analysis, is presented in [18]. The current limiting of the GFMI, which is the root cause of sequence impedance, is extensively analyzed and verified in [18] through simulations. As reported in the same paper, the control strategy of the GFMI has a significant influence on the negative sequence impedance. A different approach with electro-mechanical modeling is presented in [19] for both GFMIs and GFLIs to enable the dynamic simulation of large-scale, unbalanced distribution systems with high penetration of IBRs. The developed models are validated through simulations and field test data. The results show that high penetration of GFMIs improves the voltage and frequency stability of islanded power systems.

B. GFMI CONTROL METHODS

The common control approach for GFLIs is the vector current control. Contrary to GFLIs, the GFMIs possess the ability to form a voltage phasor at their PCC as they operate as voltage sources. The inner cascade controller structure of GFMIs is designed such that the magnitude and the angle of the voltage phasor at the PCC are dynamically controlled to achieve synchronization with the grid and support the grid if necessary. To this end, typically, a GFMI comprises multiple inner control loops such as the inner-current control loop, intermediate-voltage control loop, virtual impedance loop, active power controller (APC), and reactive power controller (RPC). The RPC and APC are used to control the magnitude and the frequency, thereby phase of the voltage at the PCC. However, it is also possible to implement GFMIs without the inner cascade loops by directly altering the inverter terminal voltage. The impact of inner cascade loops on the performance of GFMIs is reviewed in [20].

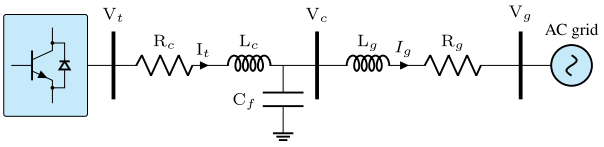

FIGURE 3. The power stage of a GFMI.

Even though the X/R ratio of the grid dictates the relationship between active power, reactive power, frequency, and voltage, typically, if the X/R ratio is high, the active power and frequency are linked together. Therefore, the APC is used to control the frequency/phase, and the RPC is used to control the magnitude of the voltage phasor at the PCC. On the other hand, if the X/R ratio is low, the reactive power is linked with frequency. Therefore, the APC is used to control the voltage magnitude, and the RPC is used to control the frequency of the voltage phasor at the PCC. If the X and R values are comparable, the frequency and voltage are coupled with both active power and reactive power. In that case, a 2×2 multi-input-multi-output controller is used to control the phase and the magnitude of the voltage phasor at the PCC. Alternatively, the impedance of the connecting line seen from the inverter can be shaped to be predominantly inductive through the use of a virtual impedance loop. Therefore, in this paper, the frequency/angle control methodologies based on the active power and voltage magnitude control based on the reactive power are reviewed. These control methodologies can be categorized into three categories, as shown in Fig. 4.

1) DROOP CONTROL

Being proposed two decades ago, droop control is the most prevalent and mature control technique out of the three categories discussed in this paper. Droop control concept originates from the governor action that enables the parallel operation of multiple synchronous generators. It is first proposed in [21] for use in isolated ac power systems and uninterruptible power supplies. Some of the earliest works on GFMIs focus on islanded power systems or uninterruptible power supplies. However, such controllers are also included in this review as they are capable of operating in large interconnected power grids. The droop control can be further categorized based on the control law as frequency-based droop control, angle-based droop control, and power synchronization control (PSC).

a: FREQUENCY-BASED DROOP

In frequency-based droop control, the frequency (ω) of the inverter is allowed to decrease linearly with the increasing P. This linear P-ω drooping behavior is defined using a droop coefficient. The transfer function for the droop control

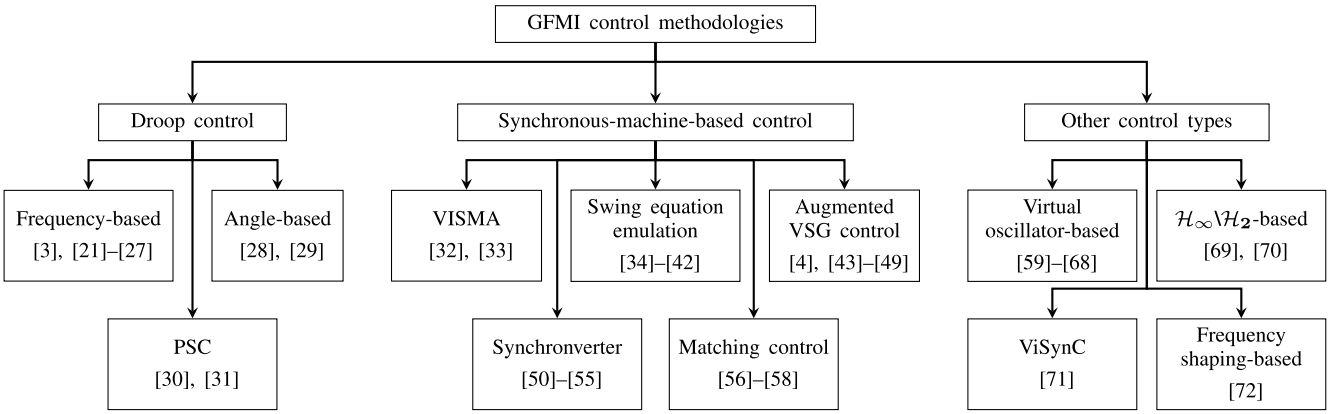

FIGURE 4. GFMI control methodologies.

(K_{Droop}) is

$$K_{\text{Droop}} = \frac{\Delta\omega}{\Delta \text{P}} = \text{K}_{\text{P}\to\omega}, \tag{4}$$

where, $K_{P\to\omega}$ is the droop coefficient. The $K_{P\to\omega}$ is chosen such that in the standalone mode, the load is shared among the inverters that are in operation based on their rating [2]. To this end, the droop coefficient is weighted based on the rating of the inverter. Fig. 5 depicts the control structure of the droop controller. Generally, to filter out the high-frequency harmonics, the droop controllers are used in conjunction with a low pass filter [22]. The control structure of a droop control with a low-pass filter is shown in Fig. 6. The transfer function of a droop controller with a low-pass filter (K_{DroopLPF}) is

$$K_{\text{DroopLPF}} = \frac{\Delta\omega}{\Delta P} = \text{K}_{\text{P}\to\omega}\left[\frac{\omega_c}{s+\omega_c}\right], \tag{5}$$

where $K_{P\to\omega}$ and ω_c are the droop coefficient and the cut-off frequency of the low-pass filter. Further, a droop control mechanism can be utilized in the RPC to control the voltage magnitude based on Q. Similar to the APC, the voltage magnitude at the PCC ($V_{\text{d,ref}}$) is linearly drooped based on the reactive power injection of the inverter. The droop based RPC is shown in Fig. 5.

The droop controlled GFMIs are capable of operating with multiple GFMIs and GFLIs in both grid-connected mode and standalone mode. The control strategies that coordinate the IBRs either utilize high bandwidth communication channels or depend solely on local measurements. The droop control only depends on the local measurements and does not require any inter-inverter communication. Thus, the implementation of droop controllers is relatively hassle-free, and redundancy is easily achieved [3]. To further improve the transient response of the classic droop control (proportional control), in [23], derivative and integral terms are incorporated into the droop controller of the active power path. In contrast, only a derivative part is incorporated into the droop control in the reactive power path. Incorporating derivative and integral terms into the droop controller overcomes the issues such as voltage deterioration with large droop gains, limited

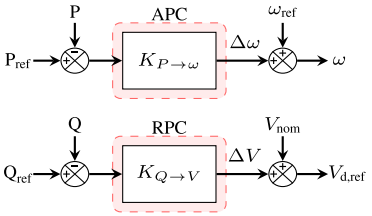

FIGURE 5. Droop controller.

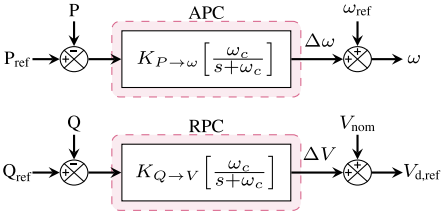

FIGURE 6. Droop controller with a low-pass filter.

power sharing accuracy, large transient circulating currents, and stability issues that are common in droop controlled inverters [23].

The conventional P-ω droop control is typically used when the connecting line is predominantly inductive. In [24], the authors have extended the classical droop control method to perform well regardless of the X/R ratio of the line. Hence, the conventional droop control is improved using a transformation matrix in [24] by taking the X/R ratio of the connecting line into account. Further, the modified droop control scheme is extended to directly control the active and reactive currents during faults instead of active and reactive powers. As an alternative approach, a virtual impedance-based approach is proposed in [25] for droop-controlled inverters operating with a complex system impedance. This method employs a virtual inductor to increase the inductive nature of the output impedance. Thus, the coupling between active power and reactive power is minimized. The virtual

impedance loop-based decoupling control is fairly intuitive, and its implementation is straightforward.

In [26], the authors have proposed an $\mathcal{H}_\infty$-based control design method to design droop controllers for the APCs of both GFMIs and GFLIs. The authors present a systematic control design framework for multiple-inverter systems that achieve robust performance with respect to various control objectives while guaranteeing global small-signal stability. The optimal controller considered in [26] is a static gain matrix that can be either a grid following controller or a grid forming controller based on the preference. To achieve the desired control objectives, the weighting functions for the corresponding sensitivity functions are chosen appropriately during the control design. In [27], a supplementary multi-variable controller is proposed for droop controlled inverters with high droop gains. High droop gains are required in inverters when the X/R ratio is low in the connecting line to improve power sharing among inverters, decrease the coupling and transient power sharing. However, high droop gains together with large loading conditions give rise to stability issues pertaining to low-frequency power modes. Therefore, a multi-variable stabilizer that operates in parallel with the droop controller is proposed. The stabilizer is designed based on Glover-Mcfarlane $\mathcal{H}_\infty$ loop shaping technique. Although the order of the resulting controller is high, it is reduced using optimal Hankel norm model order reduction method.

b: ANGLE-BASED DROOP

In [28], a phase-angle-based droop control method is proposed. The control law is presented as

$$\begin{aligned} \theta &= \theta_{\text{ref}} - m_p(P - P_0) \\ \text{V} &= \text{V}_{\text{ref}} - m_q(Q - Q_0), \end{aligned} \tag{6}$$

where θ and V are the phase-angle and magnitude of the terminal voltage, θ_{ref} and V_{ref} are the phase-angle and magnitude of the terminal voltage when the inverter is outputting rated active power (P_0) and rated reactive power (Q_0), and m_p and m_q are the corresponding active power and reactive power droop coefficients, respectively. The phase angle used in the control is relative to a system-wide reference such as the Global positioning system (GPS). Thus, no inter-inverter communication links are necessary. The m_p and m_q values are chosen based on the voltage regulation and proportional load sharing requirements.

A novel flux-based droop control method that overcomes the deficiencies in the conventional voltage-based droop control is proposed in [29]. The active power and reactive power are controlled via flux magnitude and flux angle, respectively. The proposed control law is similar to (6). However, instead of the voltage magnitude and voltage phase angle, flux magnitude and flux angle are drooped. The transient response of the system is tuned by adjusting the droop slopes while obeying the stability limits. Further, a direct flux controller is proposed to produce the reference flux generated from the flux droop controller. Thus, the cascaded inner-loops are eliminated. The proposed flux control shares the active and reactive power with less voltage and frequency deviations than voltage-based droop control.

c: POWER SYNCHRONIZATION CONTROL (PSC)

As shown in Fig. 7, a similar concept called PSC is proposed in [30] for HVDC systems to overcome the issues presented by operating vector current controlled inverters in weak-grids. Although the PSC is developed based on the operation of synchronous machines, it is categorized here mainly due to controller's structural resemblance to droop control. In the PSC, instead of the frequency, the phase angle is drooped based on the power increment. The transfer function of the PSC controller (K_{PSC}) is

$$K_{\text{PSC}} = \frac{\Delta\theta}{\Delta \text{P}} = \frac{\text{K}_{\text{P}\to\theta}}{s}, \tag{7}$$

where $\text{K}_{\text{P}\to\theta}$ is the controller gain. In PSC, the synchronization with the grid is achieved similar to a synchronous machine through transient power transfer. Even though a PLL is not required for synchronization, during faults, the PSC uses a backup PLL to switch to a GFLI.

Typically, in PSC, a DC-link voltage controller is cascaded with the active power loop. An analytical selection method for the gains of the outer DC-link controller and the active power loop of the PSC based on frequency-domain analyses is proposed in [31]. The gain for the active power loop is chosen based on an open-loop transfer function that includes the effect of the active resistance. The robustness is guaranteed by ensuring stability margins for phase (ϕ_m) and gain (g_m) margins of the open-loop transfer function are within the recommended ranges ($\phi_m \geq 45°$, $g_m \geq 2$). Since large stability margins reduce the bandwidth of the closed-loop system, the design enforces g_m to be at the minimum recommended value. Then, a weak integral action is considered for the cascaded outer-loop DC-link controller. Similar to the active power control design, the DC-link voltage controller gain is selected based on large stability margins. Thus, robustness is ensured. However, for DC-link control design, a g_m of 4 is considered so that the ϕ_m is large enough. The active power loop gain depends on the terminal voltage. Therefore, it must be gain-scheduled to account for the variation in the terminal voltage, especially during faults to avoid over-currents.

2) SYNCHRONOUS-MACHINE-BASED CONTROL TECHNIQUES

One of the serious shortcomings of the droop controller is the lack of inertia support. Therefore, novel control methodologies that incorporate the inertial and damping properties of synchronous generators are proposed.

a: VIRTUAL SYNCHRONOUS MACHINE (VISMA)

The first instance of emulating the behavior of a synchronous generator through power electronic components is introduced as a concept called *virtual synchronous machine* (VISMA) in [32]. The VISMA model is based on a complete two-shaft

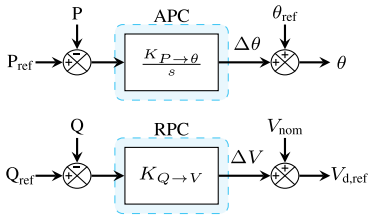

FIGURE 7. Power synchronization controller.

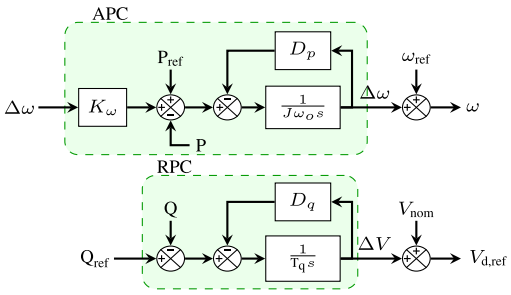

FIGURE 8. Simplified swing-based virtual synchronous generator.

synchronous machine model that includes stator windings, damper windings, and excitation windings, which are modeled in a process computer. The machine currents are calculated in real-time based on the measured voltage at the PCC and fed into the grid. The active power and reactive power are controlled based on the virtual torque and virtual excitation voltage, respectively. An upgraded version of VISMA based on measuring the grid currents instead of grid voltages and generating reference voltages instead of reference currents is proposed as VISMA-Method 2 in [33]. Following VISMA, several different control methodologies are developed to replicate the characteristics of synchronous machines in the APC.

b: SWING EQUATION EMULATION

To stabilize the frequency fluctuations in IBRs dominated grids, the VSG concept is proposed in [34]. To this end, a short-term energy storage unit and an appropriate controller are utilized to provide short-term virtual inertia for any distributed energy resource (DER) with or without rotational inertia. The *swing equation* represents the rotor side dynamics of a synchronous machine as

$$\mathrm{J}\omega_0 \frac{d\omega_r}{dt} + \mathrm{D_p}\omega_r = \mathrm{P}_m - \mathrm{P}_e, \tag{8}$$

where ω_r, $\mathrm{D_p}$, J, P_m, and P_e are angular speed of the rotor, damping constant, the moment of inertia, mechanical power, and electrical power, respectively. In basic VSG control, the control law is implemented to replicate (8). Therefore, the transfer function of the basic VSG controller (K_{vsg}) is

$$K_{\mathrm{vsg}} = \frac{\Delta\omega}{\Delta \mathrm{P}} = \frac{1}{(\mathrm{D_p} + \mathrm{k_m})} \frac{1}{\left(\dfrac{\mathrm{J}\omega_o}{\mathrm{D_p} + \mathrm{k_m}} s + 1\right)}, \tag{9}$$

where $\mathrm{D_p}$, $\mathrm{k_m}$, and J, are damping coefficient, governor coefficient, and moment of inertia, respectively. The $\mathrm{D_p}$ and $\mathrm{k_m}$ are chosen based on the desired stead-state P-ω droop, while J is chosen based on the required virtual inertia provision [35]. The control block diagram of the basic VSG control structure based on the swing equation is shown in Fig. 8. By close inspection of (9), it can be seen that the structure of K_{DroopLPF} is similar to K_{VSG} in (5). In [36], the authors have shown the droop control with a low-pass filter and the VSG are mathematically equal, and the droop control with a low-pass filter is a special case of the VSG. Also, if J and $\mathrm{D_p}$ are set to 0 in (9), it becomes similar to K_{Droop} given in (4).

A comprehensive analysis of the dynamic characteristics of droop control and VSG control is presented in [37]. In this study, both grid-connected and standalone modes of GFMIs with droop control and VSG control are considered. Then, the frequency changes during load changes in grid-connected and standalone modes are derived using the step-response of the corresponding small-signal models and electromagnetic transient (EMT) simulations. It is observed that in standalone mode, due to lack of inertia, the rate of change of frequency (RoCoF) is high with droop control compared to that of VSG control. This can cause unnecessary tripping of RoCoF sensitive equipment and load shedding. Further, it is observed that the delays in governor in VSG control amplifies oscillations and reduces virtual inertia. However, the delays in governor with droop control increase inertia [37].

One of the key advantages of the VSG over real synchronous machines is that the design parameters such as $\mathrm{D_p}$ and J can be readily changed during operation. Therefore, a bang-bang type controller is designed by tuning the inertia constant in [38] to improve post fault oscillation damping in VSGs. Further, it is shown that the alternating inertia constant control enhances the stability of the adjacent machines following a fault. A self-tuning method for the damping coefficient and the inertial constant is proposed in [39]. An online optimization-based method is used to calculate the optimal damping coefficient and virtual inertia while minimizing the frequency deviations (amplitude and rate of change both) and power flow through the energy storage system. The optimization-based self-tuning method is more efficient than the constant parameter method in reducing the frequency nadir as the self-tuning method utilizes less energy per hertz. To overcome the implementation complexity in optimization-based self-tuning method, a self-adaptive interleaving type control is proposed in [40] to tune both the inertia constant and the damping constant. A rule-based adaptive control method to tune the damping constant and inertia constant while maintaining an optimal constant damping ratio is proposed in [41]. The dynamics due to variations in damping coefficient and moment of inertia are analyzed in time-domain, and an adaptive control method is proposed.

In [42], a control algorithm that acts on short-term energy storage units to emulate the power interchange between a *virtual synchronous machine* and the grid is proposed. As shown

in Fig. 9, in this control algorithm, a PLL structure that represents a generator is used to estimate the electro-mechanical characteristics. The modified PLL behaves similar to a real synchronous machine and provides the frequency, phase, and power. The θ_s and θ_r are the phase angle of the grid-side and the inverter-side voltage of the filter inductance, respectively. The output signal y_{PD} can be calculated as

$$\begin{aligned} y_{\text{PD}} &= \text{Im}\left\{ U e^{j\theta_s} e^{-j\theta_r} \right\} \\ &= U \sin(\theta_s - \theta_r). \end{aligned} \tag{10}$$

Therefore, the control law is

$$\frac{d\omega_o}{dt} = K_p \, K_i \, U \sin(\theta_s - \theta_r). \tag{11}$$

The PLL gains K_p and K_i are chosen such that (11) resembles the transfer function of a synchronous generator. The power is then used to derive the current references for the current controller.

c: AUGMENTED VSG CONTROL

The basic VSG control is modified in many papers to achieve better damping, improved transient stability, and a better transient response. The basic VSG control is enhanced in [4] to damp oscillations, improve transient active power sharing, and share the reactive power accurately. A virtual reactance adjusting method is proposed to achieve the oscillation damping and transient power sharing, while droop control coupled with a bus voltage estimation is used to share the reactive power accurately.

The configurable natural droop (CND) controller (K_{CND}) for emulating inertia and damping is proposed in [43] to individually control inertia and damping without affecting the intrinsic P-ω droop characteristics of the VSG. In K_{CND}, instead of a first-order low-pass filter, a lead-lag controller is used to achieve the desired control objectives. The transfer function of the controller is

$$K_{\text{CND}} = \frac{\text{K}_\text{P} s + \text{K}_\text{I}}{s + \text{K}_\text{G}}, \tag{12}$$

where K_P, K_I, and K_G are used to individually tune the closed-loop bandwidth, damping coefficient, and natural P-ω droop, respectively.

In [56] and [57], the authors have presented a proportional-integral (PI) controller-based active power controller and compared the frequency support properties of that, CND control, and VSG control. Due to the integral action in the PI-based active power controller, consistently accurate power tracking is achieved, even during grid frequency variations. Further, there is no intrinsic droop as well. Therefore, the PI-based active power controller is identical to the CND controller when the K_G term is set to zero.

In [45], the authors have proposed a control method that combines the PSC and the VSG control. Further, a model order reduction method is proposed by pole/zero cancellation in closed-loop transfer functions that results in two first-order transfer function for reference tracking and droop control.

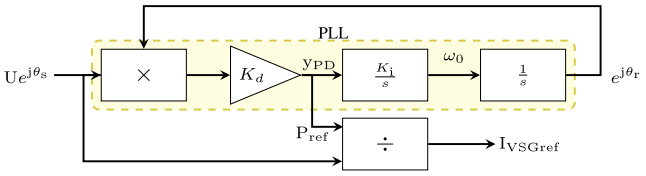

FIGURE 9. PLL that resembles a generator [42].

Therefore, the desired inertia constant and a P-ω droop can be individually set where the latter determines the closed-loop bandwidth.

Although droop control exhibits an excellent reference tracking performance, it cannot provide inertia in standalone mode. Therefore, the RoCoF becomes dangerously high following load imbalances. To prevent high RoCoFs in standalone mode, VSG control is used, and the parameters are tuned to have the desired RoCoF following load imbalances. However, this leads to large overshoots and longer settling times in grid-connected mode. Therefore, a second-order controller called generalized droop controller (GDC) based on the VSG control is proposed in [46]. The GDC results in reduced overshoots and shorter settling times in power set-point tracking in grid-connected mode while guaranteeing a desired RoCoF in standalone mode. The control design proposed to tune the gains in GDC is an onerous trial and error process.

In [47], a supplementary controller called intelligent power oscillation damper (iPOD) is added to the basic VSG control to damp the electromechanical inter-area power oscillation. The iPOD includes a bandpass filter and two proportional gains called k_1 and k_2. During the tuning process, k_1 is set to -1, and k_2 defines the amount of damping provided by the iPOD. The band-pass filter frequency corresponds to the frequency of the inter-area electromechanical power oscillation that needs to be damped. Therefore, the band-pass filter frequency is set based on a real-time prediction obtained from an artificial intelligence-based predictor that employs the Random Forest algorithm. Due to the structure of the controller, the iPOD adds an additional phase margin around the inter-area electromechanical power oscillation frequency.

Typical GFMIs are capable of providing various control functionalities such as virtual-inertia provision, active power reference tracking, and frequency support in the steady-state. In [48], a PLL-free APC design is proposed to decouple different control functionalities of the GFMIs. Such a decoupling of control functionalities is beneficial for the GFMI owner so that they can opt out from frequency support. A proportional term of the active power output is added to the integral of the error between power reference and output power (which defines the virtual-inertia provision). The proportional term adds additional damping, and it is tuned based on a desired closed-loop damping ratio. The integral gain is set based on a desired virtual inertia provision. The v_{PCC} is stiffly controlled, and a reactive power droop is used if necessary. The proposed grid forming control method is integrated

with the cascaded inner voltage and current loops where a current saturation controller and a transient virtual impedance loop are employed for better transient response. The proposed method achieves good inertial response, robustness towards grid-parameter changes, and good voltage regulation at PCC.

In [49], the authors have presented a fuzzy-based method to dynamically adjust the inertia of the VSG during transients by altering the power output of the governor. Contrary to online-tuning of inertia and damping constant methods, the fuzzy controller utilizes the rotational angle, angular frequency, and rate of change of frequency to improve the inertial response. One of the main drawbacks of fuzzy control is that fuzzy rules heavily depend on the designer's knowledge of the system. Consequently, the fuzzy membership characteristics and fuzzy rules significantly affect the performance of the controller. Further, the Mamdani fuzzy inference used in [49] is computationally intensive compared to other inference systems such as Takagi-Sugeno inference. Computational burden is critical in improving inertial response as the time-scale of operation is very low.

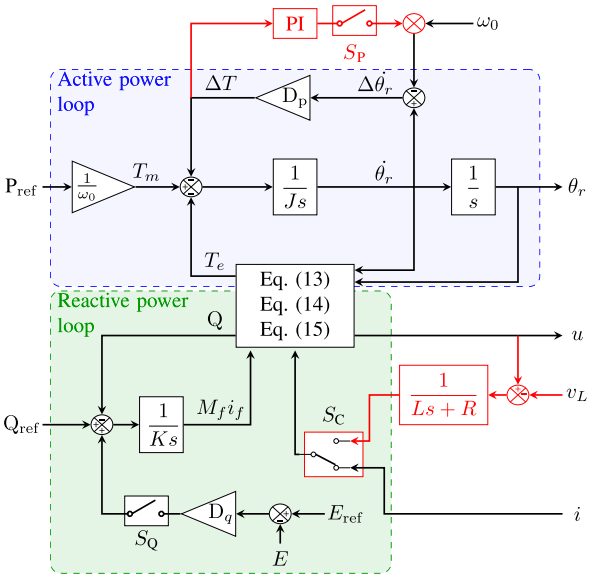

FIGURE 10. Control block diagram of the Synchronverter [51].

d: SYNCHRONVERTER

Another synchronous machine emulating control method is the Synchronverter. The concept, control, and implementation of Synchronverter is first proposed in [50]. The Synchronverter mimics the behavior of a synchronous generator. Therefore, when a Synchronverter is connected to the grid, the dynamics seen from the grid-side is equivalent to the dynamics coming from a synchronous generator. One of the key advantages of the Synchronverter over the synchronous generator is that parameters such as inertia, damping, field inductance, and mutual inductance can be readily tuned. The control block diagram of a Synchronverter is shown in Fig. 10.

The electromagnetic torque (T_e), back electromotive force (EMF) (u), and reactive power (Q) are calculated as

$$T_e = M_f i_f \langle i, \widetilde{\sin(\theta_r)} \rangle \tag{13}$$

$$u = \dot{\theta}_r M_f i_f \widetilde{\sin(\theta_r)} \tag{14}$$

$$Q = -\dot{\theta}_r M_f i_f \langle i, \widetilde{\cos(\theta_r)} \rangle \tag{15}$$

$$\widetilde{\sin\theta_r} = \begin{bmatrix} \sin(\theta_r) \\ \sin(\theta_r - \frac{2\pi}{3}) \\ \sin(\theta_r + \frac{2\pi}{3}) \end{bmatrix}, \quad \widetilde{\cos\theta_r} = \begin{bmatrix} \cos(\theta_r) \\ \cos(\theta_r - \frac{2\pi}{3}) \\ \cos(\theta_r + \frac{2\pi}{3}) \end{bmatrix} \tag{16}$$

where M_f, i_f, i, θ_r, and $\langle \cdot, \cdot \rangle$ are peak value of mutual inductance, rotor excitation current, stator phase currents, rotor angle, and conventional inner product, respectively. The parameters D_p and J in the active power loop are set based on the steady-state P-ω droop and desired virtual-inertia provision, respectively. The parameters D_q and K in the reactive power loop are chosen based on the steady-state Q-V droop and voltage loop time constant, respectively.

Typically, the frequency reference, voltage reference, and phase reference for the controller are provided by a dedicated synchronization unit. Therefore, to overcome the reliance on a dedicated synchronization unit (e.g., PLL), self-synchronization ability is added in [51] by driving the error between the internal frequency and grid frequency to zero using a PI controller. This is shown in Fig. 10 as the operation of the switch S_P. The stability margin of the conventional Synchronverter around 50 Hz is increased in [52] by a filter-based current feeding method. Thereby, the power ripples at 50 Hz are eliminated. Further, the operation of the conventional Synchonverter under an unbalanced grid is analyzed. A modified Synchronverter with a multi-input multi-output controller is proposed to eliminate power ripples and prevent current harmonics. A second-order generalized integrator-based resonant controller is used to suppress the double frequency current oscillations in the synchronous frame.

In [53], the authors have proposed designing an additional damping loop to improve the damping without affecting the intrinsic P-ω droop. An additional feedback loop of the rate of change of torque is used to implement the additional damping loop. In [54], the authors have proposed a method to directly tune the Synchronverter parameters, including the additional damping loop, by considering a reduced third-order system that captures the pertinent dynamics of the active power loop. The parameters of the Synchronverter are chosen based on the desired natural frequency and damping of the dominant mode of the active power loop. The proposed method simplifies the tuning process by avoiding strenuous trial and error tuning and repeated calculation of system eigenvalues. The authors in [55] have proposed a pole placement control design method based on the desired closed-loop performance. First, a reduced third-order model of a VSG that takes the effects of

an inductive and resistive weak grid into account is derived. The parameters such as damping and inertia constant of the VSG are calculated based on the desired placement of the closed-loop poles. To increase the damping, an additional damping loop, as proposed in [53] is designed.

e: MATCHING CONTROL

In [56], [57], the authors have presented a novel GFMI control strategy called matching control to match the electromechanical energy transfer of synchronous machines by utilizing the DC-link voltage, not only as a pivotal control signal but also as a proxy signal for power imbalances. The complete electronic realization of the synchronous machine (eSM) and control design based on energy shaping techniques is proposed in [58]. Contrary to numerical synchronous machine emulation methods, the authors propose an exact physical realization of the synchronous machine by utilizing the integral of DC bus voltage measurement as the internal angular frequency of the voltage source inverter. Therefore, the physical quantities of synchronous machines such as the moment of inertia, rotor damping coefficient are represented by analogous physical quantities of the voltage-source inverter. Both grid following and grid forming control are realized using two separate energy functions. In the grid forming control scheme, it is shown that droop control acts as the synchronization toque. To compensate for the model inaccuracies and uncertainties, a proportional resonant controller is used in parallel to matching control.

3) OTHER CONTROL METHODOLOGIES

Apart from the conventional droop control and synchronous machine-based control, several other control methods are developed for GFMIs. Although some of these are based on linear control design techniques, most of them are based on nonlinear control design techniques.

a: VIRTUAL OSCILLATOR-BASED METHODS

Virtual oscillator control (VOC) is a nonlinear control technique proposed in [59] to control the inverters to mimic the dynamics of a weakly nonlinear oscillator. A single dead-zone oscillator which includes a parallel connection of a virtual resistor, inductor, capacitor, and a voltage-dependent current source is used as the nonlinear oscillator. The scaled quantities of the inverter current and the capacitor voltage are used to implement the VOC. The capacitor voltage is used as the control signal in the pulse width modulation (PWM) to produce the terminal voltage. One of the key advantages of the VOC is that the parallel-connected inverters are able to synchronize with each other without any inter-inverter communication. To this end, a sufficient condition for synchronization based on the Euclidean norm of a function based on the filter impedance, the impedance of the passive components of the nonlinear oscillator, and the capacitor voltage and inverter current scaling factors is derived. The control design is based on iterative open-circuit and full load tests while ensuring the selected control parameters satisfy the sufficient condition for synchronization. The VOC control is extended to three-phase microgrids in [60] under the assumption of a stable, balanced three-phase grid. Further, an MPPT method is formulated to integrate with VOC to form a photovoltaic (PV) inverter.

In [61], a Vander Pol oscillator is considered as the weakly nonlinear limit-cycle oscillator for VOC, and a systematic design process, as opposed to iterative open-circuit and full load tests, is proposed to achieve the desired frequency and voltage regulation specifications. The controller is a discretized version of the Van der pol oscillator, which includes a parallel connection of a virtual inductor, capacitor, conductor, and a cubic voltage-dependent current source. Scaled quantities of the capacitor voltage and inverter current are used to implement VOC. The scaled capacitor voltage is used as the control signal in the PWM stage to synthesize the terminal voltage. The frequency of the terminal frequency is equal to the resonance frequency of the inductor-capacitor resonant frequency of the Van der pol oscillator. The parameters in the Van der Pol oscillator and the scaling terms are tuned based on the desired performance specifications. The proportional power sharing between multiple inverters is ensured by properly choosing the scaling factors for capacitor voltage and inductor current. The conductance and coefficient of the cubic voltage-dependent current source are tuned based on the desired voltage regulation specifications, while the inductance and capacitor values of the harmonic oscillator are chosen based on the frequency regulation specifications, rise time, and harmonic performance.

The authors in [62] have studied the dynamics of inverters that are designed to mimic the dynamics of Van der Pol oscillators. The authors have considered resistive islanded microgrids and compared Van der Pol oscillator dynamics with the droop laws that are based on the average active and reactive powers. This facilitates the design of Van der Pol oscillators based on the optimal droop gains for load sharing and economic optimality in the steady-state. Further, the authors have studied the stability of the average voltage amplitude and phase dynamics in microgrids with resistive interconnecting lines and identified a set of desirable equilibria.

Based on the previously published work on VOC, the authors in [63] and [64] have developed a dispatchable VOC (dVOC), which is capable of obtaining power and voltage set-points and driving the electrical power system to a required power flow solution instead of a trivial one. Further, it is shown that the controller guarantees almost global asymptotic stability under a mild stability condition. In [65], the authors have extended the stability analysis of dVOC considering the dynamics of transmission lines. Explicit boundaries on the controller set-points, gains, and branch power flows that guarantee the global asymptotic stability are derived.

A hierarchical control structure is proposed in [66] for a VOC dominated micro-grid for operation and seamless transition between standalone and grid-connected modes.

An integral controller is proposed as the secondary controller to match the voltage magnitude, frequency, and phase at the PCC to those of the bulk grid. Further, to mitigate the third harmonic in grid-connected operation, a notch filter is used at the output of the harmonic oscillator. In grid-connected mode, tertiary level integral controllers are designed to track active and reactive powers by each inverter in a VOC dominated micro-grid. A significant third harmonic distortion in voltage is caused by Van der Pol oscillator-based VOC implementations. A notch filter-based method is used in [66] to mitigate the third harmonic distortion although, notch filter-based method is ineffective in suppressing harmonics coming from the grid-side. Therefore, a virtual impedance-based method is proposed in [67] for selective harmonic current rejection. The converter output impedance is shaped to have a high gain around the harmonic frequencies to suppress the harmonic grid currents. A grid-side current feedback is used to implement an inductive virtual impedance that facilitates minimal nonpassive regions around resonance frequencies in converter output impedance.

A unified voltage oscillator controller (uVOC) is proposed in [68] to facilitate the unified analysis, design, and implementation of GFMIs and GFLIs. The fault ride-through capability of dVOC is improved in uVOC by enabling synchronization with low grid voltage and incorporating fast over-current limiting. In uVOC, the grid following mode is realized without a PLL unit. Instead, a space vector oscillator is used to achieve synchronization. The space vector oscillator comprises a harmonic oscillator, magnitude correction, and synchronization feedback. In grid following operation magnitude correction factor is set to zero. Harmonic oscillator rotates the voltage vector at a nominal frequency while the synchronization feedback term realigns and adjusts the voltage vector to track the power references. In the grid forming mode, the magnitude correction term naturally engenders a droop like behavior to adjust the voltage.

b: $\mathcal{H}_\infty\backslash\mathcal{H}_2$-BASED ROBUST FIXED-STRUCTURE CONTROL

In [69], a robust fixed-structure control design method is proposed for synchronous oscillation damping in low-voltage and medium-voltage power grids. The proposed robust control design method is capable of working with both parametric and experimentally identified non-parametric models of the system. In the control design, the performance and stability specifications are defined as constraints on the ∞-norm of the sensitivity functions, and the optimization problem is solved iteratively until an optimal controller is reached. The robust fixed structure control design is extended to distributed control in [70]. The control design is based on an experimentally identified frequency response, and the order of the controller is not restricted, and it is up to the designer. The frequency and voltage control performance requirements are formulated as frequency domain constraints on the two-norm of the weighted sensitivity functions. A linear matrix inequality-based optimization problem is solved to obtain the optimal controller gains. The controller improves frequency and voltage transient performance while guaranteeing stability for fixed communication delays.

c: VIRTUAL SYNCHRONOUS CONTROL UTILIZING DC-LINK CAPACITOR DYNAMICS (ViSynC)

In [71], the authors have proposed a DC-link controller that is capable of both grid synchronization and DC-link voltage tracking. The basic control law is

$$\omega = \omega_g + \frac{s + \mathrm{k}_T}{\mathrm{k}_J s + \mathrm{k}_D}\left[(\mathrm{V_{DC}})^2 - (\mathrm{V_{DC}^{ref}})^2\right], \tag{17}$$

where ω, ω_g, k_T, k_J, k_D, $\mathrm{V_{DC}}$, and $\mathrm{V_{DC}^{ref}}$ are internal frequency of the GFMI, frequency setting value, damping coefficient, inertia emulation coefficient, DC-link voltage tracking coefficient, DC-link voltage, and DC-link voltage reference, respectively. It is shown that (17) together with the DC-link plant model form a model that resembles (8). Therefore, ViSynC enabled GFMIs hold similar power-frequency characteristics to synchronous generators. The damping and inertia are carefully tuned using k_T and k_J such that the DC-link voltage deviation under grid frequency changes is acceptable. The voltage management is done by simply adopting a Q-V droop controller.

d: FREQUENCY SHAPING-BASED CONTROL

A novel frequency shaping-based control technique is proposed in [72] to aggregate the center of inertia frequency dynamics in a low-inertia system to a first-order response. Thus, a large overshoot that could have caused an undesirable frequency nadir is avoided. The proposed control technique allows a desired steady-state frequency deviation and RoCoF during power imbalances. A second-order controller is used in GFMIs. The controller gains are tuned either by matching individual turbine dynamics by individual inverter or distributing the weighted aggregated first-order response of turbines across all the inverters. The second approach is seen as more practical as it does not require the knowledge of each individual turbine dynamics.

C. COMPARISON BETWEEN DIFFERENT GFMI CONTROL METHODOLOGIES

The GFMI control methodologies reviewed in this paper are unique in their own right. Each of them has distinct characteristics and features that set it apart from the other controllers. Therefore, a comparison of different features of different GFMI controllers is useful to researchers and power system engineers. To this end, Table 2 shows a comparison between different GFMI control categories, as shown in Fig. 4, based on various features such as tunable virtual inertia, PLL for synchronization, overcurrent protection, communication-less control, and dispatchability.

Virtual inertia provision capability is an important aspect of GFMI control methodologies. Typically, virtual inertia is a control design parameter in GFMIs as opposed to a physical parameter as in synchronous machines. Therefore, tunable virtual inertia corresponds to the ability to tune the

TABLE 2. Comparison between different grid forming control methodologies.

Category	Control structure	Tunable virtual inertia	PLL for synchronization	Overcurrent protection	Communication-less	Dispatchable
Droop-based	Frequency droop [22]	✗	✓	✓	✓	✓
	Angle droop [28]	✗	✓	✓	✗[1]	✓
	PSC [30]	✗	✓	✓[2]	✓	✓
Synchronous machine-based	VISMA [32]	✓	✓	✓	✓	✓
	VSG [35]	✓	✓	✓	✓	✓
	CND [43]	✓	✓	✓	✓	✓
	GDC [46]	✓	✓	✓	✓	✓
	Synchronverter [50]	✓	✓	✗	✓	✓
	eSM [58]	✓[3]	✗	✓	✓	✓
Other methods	VOC [59]	✓	✗	✗	✓	✗
	$\mathcal{H}_2/\mathcal{H}_\infty$ [69]	✓	✓	✓	✗[4]	✓
	ViSynC [71]	✓	✗[5]	✓	✓	✓
	Frequency shaping [72]	✓	✓	✗	✗[6]	✓

1- GPS is required for angle reference [28].
2- During severe grid faults control system switches to PLL-based vector current control [30].
3- Extra inertia and damping is provided by the upstream converter [58].
4- PLL is used to detect the steady-state frequency [71].
5- Communication networks are required for distributed control. [69].
6- Deriving first order aggregate turbine dynamics require some format of communication. [72].

inertia based on the objectives of the designer. As shown in Table 2, droop-based control methodologies do not possess the virtual inertia provision capability as they are generally high-bandwidth controllers. On the other hand, the majority of the synchronous machine-based control methodologies are capable of providing virtual inertia. In eSM, inertia and damping are directly related to capacitance and parallel conductance of DC-link, respectively. This is due to the exact physical realization of a synchronous machine done in eSM as opposed to a numerical realization. Therefore, inertia and damping are tied to the physical parameters of the GFMI. However, additional inertia and damping can be provided by the upstream converter through the control of DC-link current.

For a smooth grid-synchronization, the voltage difference in terms of amplitude, frequency, and phase at the PCC and grid should be minimum. To this end, typically, droop-based and synchronous machine-based GFMI control methodologies require a synchronization unit (e.g. PLL) to synchronize to the grid although, the synchronization unit is not required during operation as synchronism is preserved by the power controller. This is analogous to the synchronization process prior to the grid connection used for synchronous machines. This deficiency in Synchronverters is overcome using a PI controller in [51]. Global asymptotic synchronization for a virtual oscillator controlled microgrid is proposed in [59]. A secondary control strategy is proposed in [66] to enable grid-synchronization and seamless transition.

As shown in [73], typically, droop-based or synchronous machine-based GFMIs can be implemented either with the inner-loops (voltage and current) or without the inner-loops. If the GFMIs are implemented with the inner-loops, the over-current protection can be facilitated by limiting the current references to the inner-current loop. The Synchronverter is first proposed without the use of inner-loops [50]. Nevertheless, over-current protection can be added by simply adding an inner-current loop. The earliest virtual oscillator-based methods also lack over-current protection and fault-handling capabilities. However, over-current protection is proposed for virtual oscillator-based controllers in [68].

One of the major advantages of frequency-based droop control is the ability to operate solely based on local measurements. In contrast, the angle-based droop control requires an angle reference. Angle reference is provided by the signals from GPS. However, no inter-inverter communication is necessary for angle-based droop. Similar to frequency-based droop control, synchronous machine-based and other GFMI control methods do not require communication networks for operation. However, frequency shaping-based control strategies require some forms of a communication network to identify the first-order aggregated turbine dynamics during the control design stage. Further, the multi-input multi-output $\mathcal{H}_2/\mathcal{H}_\infty$-based control design framework supports centralized, decentralized, and distributed control design for GFMIs. The centralized and distributed controllers require communication networks for communication between the inverters. However, decentralized controllers do not require a communication network.

The term dispatchability refers to the ability of a controller to follow the power and voltage reference commands received from the automatic generation control (AGC). All of the controllers reviewed in this paper possess this ability except the VOC proposed in [59]. However, this is overcome in [63], [64], and it is called dVOC.

IV. GRID FORMING INVERTER CHALLENGES

A. STABILITY ANALYSIS

Stability analysis of GFMIs is an important area that has drawn increased attention in recent years. The analysis reported in the literature can be classified into small-signal stability analysis and transient stability analysis. More

information on the two categories is given in the following subsections.

1) SMALL-SIGNAL STABILITY

The authors in [74] present fundamental insights on understanding the small-signal stability of low-inertia systems with both grid forming and grid following inverters and their interaction with various components of the power system at various time scales, as shown in Fig. 11. The study indicates that the main difference between conventional and low-inertia systems is the timescale separation between the respective controllers of synchronous generators and IBR, which leads to instability under high penetration. The study also determines the most vulnerable segments of the system and provides directions for improving the stability margin under different generation portfolios.

A region-based small-signal stability analysis approach is presented in [75], which requires a detailed model of the GFMI controller and its parameters. The region-based technique is able to analyze the impact of high penetration GFMIs and GFLIs and the effects of controller parameters variation. However, the implementation of region-based stability analysis becomes complex when the number of GFMIs is increased. As an alternative, a μ-analysis method is proposed in [76]. In this method, the system equations are linearized around an operating point of interest. The impact of grid condition and controller parameters are investigated by μ-analysis. The concept of robust stability analysis of a GFMI in a power system is widely used in different studies [77], [78]. In [77], the performance and stability of a synchrovonverter are analyzed with the μ-analysis method, and in [78], the interaction of a GFMI with a power system and a GFLI is studied.

In [79], a complex system is divided into different subsystems, and the synchronization stability of parallel inverters based on each model sub-system is investigated. This method can be used on different kinds of inverters, such as GFMIs. The stability of a GFMI connected to a system can be guaranteed if each inverter has a passive synchronization behavior, which means the frequency-power characteristic of each GFMI impedance has a positive real value for all the frequency ranges. Moreover, the effects of the inner control loops of a VSG on its output impedance are taken into consideration in the stability analysis in [80]. The study in [80] reveals the adverse impacts of the inner loops on the system stability. Furthermore, the relations between the control parameters in the inner loops and the VSG's output impedance are also studied in this work. In [81], based on the impedance-based stability analysis, the stability of a GFMI is investigated in a weak and a strong system. The stability of GFMI is compared to a GFLI in a weak system. It shows that in a stiff grid, GFMIs can introduce instability challenges.

Positive impacts of GFMIs on the power network stability are investigated in [82] by means of the eigenvalue decomposition technique and the graph theory. In [82], it is mathematically shown that the grid strength, measured by the general short circuit ratio (gSCR) [83], from the point of view of a GFLI, is enhanced if GFMIs are installed in the network. The authors of [82] also propose two heuristic algorithms to determine optimal locations for the GFMI installations, with the objective of maximizing the smallest gSCR in the network. However, the dynamics of the reactive power control of GFMIs is not included in this study. Besides, more constraints, e.g., frequency stability, are expected to be considered for the GFMIs' location optimization.

2) TRANSIENT STABILITY

Grid frequency stability with the massive integration of GFMIs, up to 100%, is studied with EMT simulations in [84]. It is reported that at increased levels of penetration, there can be interactions with power system stabilizers (PSS), and re-tuning of the PSS is required to maintain system stability. Another observation made is that, with high penetration of GFMIs, the grid dynamics change drastically, impacting the system frequency nadir and RoCoF. This would imply rethinking of protection devices and load shedding schemes. The authors in [85] and [86] have studied the interaction of GFMI with synchronous machines and the impact of GFMI on frequency stability. With different grid forming control techniques, the studies highlight the positive impact of GFMI on frequency stability and analyze the limitations of the fast-acting controls of GFMI when interacting with the slow dynamics of synchronous machines.

The authors in [87] present a transient stability analysis of GFMIs with a single-loop voltage-magnitude (SLVM) control scheme using phase portrait analysis. Compared to GFMIs using vector-voltage control, where the transient stability is dominated by outer power control loops, the use of SLVM has shown to have a critical impact on transient stability. The authors in [88] have studied the problem of P-f droop controlled GFM inverters in losing synchronism (synchronous instability) under large disturbances. The analysis of virtual power angle characteristics shows that current limitations can lead to complicated instability mechanisms and greatly decrease the stability margin.

The authors in [89] propose impedance-based modeling of grid forming VSG in synchronous inertial reference coordinates (SIRC) to measure the voltage stability of weak grids. Moreover, frequency dynamics are also analyzed by proposing a motion equation, where the stiffness is defined to illustrate the synchronizing capability of VSG with weak grids. Large-signal stability of GFMI and GFD VSG are compared using energy function modeling by the authors in [90]. The results show that compared to a GFMI, the GFLI loses stability by exhibiting a varying damping coefficient. The indicator of the equivalent damping can be used as a criterion of whether the grid forming/following control is suitable for the weak/strong grid condition. The authors in [91] investigate the transient angle stability of GFMI (VSG) using Lyapunov's direct method, and they study the influence of different control parameters on the angle stability and propose an improved control method. In addition, apart from

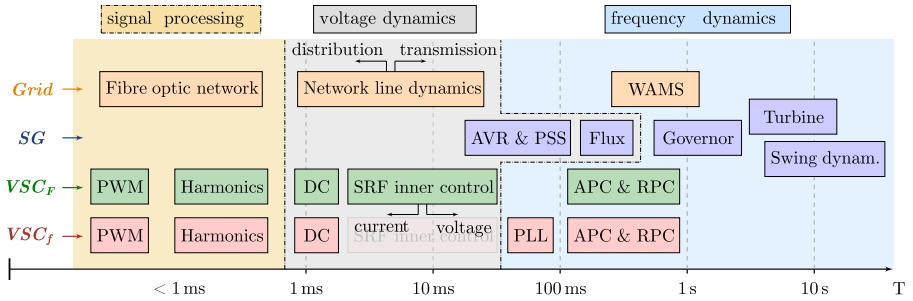

FIGURE 11. **Overview of time scale difference in different physical and control dynamics, for stability considerations [74] *(Copyright © 2021, IEEE)*.**

employing the Lyapunov theory to investigate the transient stability of GFMIs, sub-transient and transient impedances of GFMIs are obtained in [92].

Different GFMI controls behave differently in faults and voltage sag events. The studies in [93] and [94] show that the non-inertial controls, e.g., frequency-based and angle-based droop controllers, experience a first-order transient under a fault or a voltage sag. The angle transient of the non-inertial controls is smooth and overshoot-free. Moreover, the first-order power-angle dynamic of the non-inertial controllers allows the GFMI to recover from a fault even when the critical clearing time is exceeded [93], [95]. On the other hand, overshoots and oscillations can be observed in the power angle and the active power transient of inertial GFMIs, e.g., VSGs and synchronverters, under and after voltage sag conditions or load fluctuations [93], [96], [97]. The overshoot in the power angle may exceed the unstable equilibrium point of the GFMI, hence resulting in angle instability after a fault.

The overshoot and oscillation damping can be improved by adjusting the droop coefficient and the inertia constant [93], [97]. However, these two parameters are usually designed based on the grid regulations. Thus, additional damping mechanisms are required. A dynamic virtual resistance model, which is further discussed in Section IV-C2, is proposed in [96] to dampen the post-fault oscillations. However, the virtual resistance is not an effective solution for enhancing oscillations caused by loading fluctuations [97]. Instead, a virtual damping control and a virtual reactance model are introduced in [97] to suppress the power oscillations of paralleled synchronverters during load disturbances. In [98], a similar virtual damping control is integrated into the active power control loop of VSGs to dampen post-fault oscillations. Unlike the proposal in [97], which employs a high-pass filter to detect frequency transients, this damping control utilizes a PLL for the same purpose. These virtual damping methods are disabled in the steady-state operation of VSGs.

In addition, a graphical method is introduced in [95] to study the transient stability of uVOCs under various grid fault scenarios. Moreover, this work considers the effects of voltage dynamics and current limitation during large-signal disturbances when investigating the transient stability. Besides, a graphical stability analysis for dVOCs, called vector field on the circle, is introduced in [99]. By examining a droop-based and a dVOC GFMI under various grid fault conditions, [99] concludes that the dVOC outperforms the droop-based control in terms of transient stability. Additionally, it has been shown that during a voltage disturbance, voltage drops caused by the reactive power control result in adverse impacts on the transient stability of droop-based control, VSG control, and dVOC [93], [99].

The interactions between GFMIs and external assets, e.g., transmission lines, GFLIs, and SGs, in large-signal disturbance events, e.g., faults, are also investigated in the literature. More details are presented below.

The authors in [65] have studied the effect of transmission line dynamics on GFMI control, specifically the dispatchable virtual oscillator control (dVOC). The study shows that the transmission line dynamics have a destabilizing effect on the multi-inverter system, and the gains of the inverter control need to be chosen appropriately. The proposed stability condition quantifies how large the time-scale separation between the inverters and the network needs to be to ensure stability. The authors in [100] have investigated the transient stability and stability-oriented control design for the parallel operation of GFMI and GFLI in fault scenarios. With the developed mathematical model of the parallel system, transient stability is analyzed through extended equal area criteria, and improved control is achieved. This study also discusses the impacts of the current injection provided by GFLIs during faults on the transient stability of GFMIs.

Additionally, the authors in [101] study the transient angle stability of a parallel-connected synchronous generator and GFMI (VSG) by comparing it with that of the paralleled GFMIs. It is found that the GFMI and synchronous generator combination is more prone to instability due to the larger acceleration area during and after a fault compared to the case of paralleled GFMIs. This is a result of the difference in the governor's speed of SGs and GFMIs. The authors also propose a control method to improve transient stability. Apart from that, the power oscillation caused by the mismatch in line impedance and inertia between parallel synchronverters during loading fluctuations is studied in [97]. A virtual

reactance model is proposed by the authors to adjust the line impedance, hence mitigating the oscillation.

B. STANDALONE AND GRID-CONNECTED MODE TRANSITION

In the grid-connected mode of operation, inverters are controlled to inject a certain amount of current into the grid depending on the reference set by an MPPT algorithm or a reference provided by a central controller. The inverter is operated in a grid-feeding mode, as the reference voltage and frequency are established by the upstream grid. However, in an islanded mode of operation, e.g., a microgrid with local generation and loads, it is crucial to have some of the IBRs to operate in a grid forming strategy to regulate the local voltage and frequency. Hence, a seamless transfer of operation between the GFMI and GFLI modes of operation is essential in such a situation. The two main challenges in obtaining a seamless transfer of operation are fluctuation in frequency and deviation in voltage and currents.

Reference [102] develops a phase adjustment technique to minimize poor transients caused by transiting from the islanded to the grid-connected mode, namely *smooth frequency variation technique*. A comparison with other phase adjustment methods is also included in [102]. In [103], the role of PLL in enhancing the mode transitions is emphasized. From the grid-connected to the islanded mode, the PLL provides the load voltage controller with an initial power angle value. Besides, a pre-synchronization process is implemented by the PLL before connecting the inverter to the main grid. However, it is worth noting that the inverter operates as a PLL-based GFLI in the grid-connected mode. A similar approach is presented in [104]. However, in [104], a rate limiter is applied to the voltage reference to obtain a smoother transition in the output voltage when the inverter is re-synchronized with the utility grid. Additionally, the authors of [105] propose a predictive control, along with a synchronization and a phase jump adjustment algorithm, to enhance the mode transitions. The above proposals require a PLL for the re-synchronization process.

In contrast, no PLL is needed to implement the adaptive internal mode-based controller, as proposed in [106]. Moreover, by continually learning about the environment and adjusting its parameters, this controller results in smooth mode transitions. Besides, in [106], the inertial VSG control is utilized in both the islanded and grid-connected mode. Additionally, the authors in [107] propose a modified linear voltage control strategy and a modified droop mechanism to obtain a smooth mode transition.

For microgrids consisting of multiple inverter-based distributed generators, a dedicated inverter, called the principal inverter that is directly connected to the utility grid, provides other inverters, known as auxiliary inverters, with mode transiting commands, i.e., voltage and phase anglereferences [108]. In addition, all the switches inside the principal inverter are switched off during the mode transitions. Detailed state machines of the principal and the auxiliary inverters are provided in [108]. The proposal in [109] also requires a dedicated inverter to re-synchronize the microgrid with the utility grid. However, in [109], the synchronizing inverter remains in a voltage-based droop control in both modes. This helps avoid severe transients caused by changing the whole control structure during the mode transitions. Also, the regulations of the inverter voltage, frequency, and phase angle to the counterparts at the PCC are necessary and discussed in [109]. In addition, a PLL is required for the re-synchronization process in [109].

The paper discusses some of the most relevant and common proposals for enhancing the mode transitions. A more detailed review of this topic is presented in [110].

C. OVER-CURRENT PROTECTION AND FRT

Operating as a voltage source, GFMIs maintain the v_{PCC} at its set-point. As a result, during faults and voltage sags, they have to inject a large amount of current to the grid to bring v_{PCC} back to the set-point. Unlike synchronous machines, which can handle up to 6-7 per unit (pu) of over-current, semiconductor switches inside the GFMI can tolerate only 20%-40% of over-current without oversizing [111]. High over-current can lead to the failure of the switches due to the short thermal time constant of the semiconductor [112]. Therefore, a current limitation mechanism is necessary for protecting GFMIs from over-currents. Various current limiting methods have been proposed in the literature. In general, these methods can be categorized into two main groups: current-controlled and voltage-controlled limiters. In addition, current limitations during asymmetrical faults are also presented in this section. Finally, the fault recovery process of GFMIs is discussed at the end of this section.

1) CURRENT LIMITATION

a: CURRENT-CONTROLLED LIMITER

The methods discussed in this group change the voltage-controlled mode of a GFMI to a current-controlled mode when over-currents are detected. During a fault, the current control is prioritized over the voltage control to precisely limit the over-current within an allowable range. There are two main subcategories in the current-controlled group, which include grid following control [113]–[117] and current saturator [96], [118], [119].

Regarding the grid following control, when a fault occurs, the inverter is switched to the grid following mode and operates as a current source, hence losing the grid forming ability. In this mode, the output current of the inverter is controlled to track a pre-defined fault current waveform [113], [114], [117]. The pre-defined fault current reference guarantees that the over-current is within a permissible range. In addition, a backup PLL is required to keep the inverter synchronizing with the grid [116]. However, PLLs do not perform effectively in weak grids and voltage sag conditions [120], [121]. Besides, operating as a current source during a fault results in a shift of the fault power-angle curve. This reduces the overlap

between the steady-state and the fault power-angle curves of the inverter. Hence, the chance of recovering to the pre-fault operating point diminishes [119].

Another alternative for limiting over-current is the current saturator or current saturation algorithm (CSA). Unlike the aforementioned mode-switching method, a PLL is not needed for implementing the current saturator. The CSA can be inserted between the voltage control loop and the current control loop of a GFMI, as shown in Fig. 12. When the output current exceeds a threshold value, the inverter output current-set-points, i.e., $i^*_{d,ref}$ and $i^*_{q,ref}$, saturate to their corresponding maximum values [118], [119]. The saturated current-set-points, i.e., $i_{d,ref}$ and $i_{q,ref}$, are fed to the current control loop. Different CSAs, which determine the maximum current-set-points, are presented in [118], including DQ component limitation, vector amplitude limitation, and setting saturated values.

If the control is implemented in an α-β frame, saturating the sinusoidal current waveform results in distortions in both the output voltages and the output currents of the inverter [122]. These distortions can be avoided by using the circular current saturator proposed in [95] and [96]. Similarly to the grid following control, the inverter with the CSA behaves as a current source during over-current scenarios. Hence, the problem relating to the shift of the power-angle curves, as mentioned in [119], might occur when the current saturates. Apart from that, windup can degrade the transient responses during and after the fault [123]. Moreover, windup can even lead to instability [124]. Overall, current-controlled limiters allow precisely limiting the output current within a permissible range. However, these methods switch the GFMI to a current-controlled source, leading to several severe problems as aforementioned.

b: VOLTAGE-CONTROLLED LIMITER

This method helps the GFMI remain in a voltage-controlled mode as in the normal operation. Virtual impedance (VI) is the key element used for limiting over-currents, yet still operating the GFMI as a voltage source. Various models of VI have been proposed and studied in the literature [122], [125]–[127].

As shown in Fig. 12, the VI is usually implemented in the GFMI control by subtracting the virtual voltage drops over the VI, i.e., δv_d and δv_q, from the voltage references generated by the Q-V droop, i.e., $v_{d,ref}$ and $v_{q,ref}$ [122], [124]. However, due to the slow dynamics of the voltage control in the cascade control loops, there is a delay for the VI to actually become effective on the output currents. This delay can be reduced by adding another virtual-voltage-drop subtraction to the terminal voltage calculation, as presented in [126]. However, assuming PI controllers are used in the current control loop, disturbing the terminal voltages, which are the outputs of the current controller, can lead to windup. Hence, anti-windup is required for the PI controllers in the current control loop.

Most of the VI methods operate in a trigger-reset manner. The VI is only active during a fault and deactivated in the normal operation. A static VI model is proposed in [127]. Although a short amount of time is given for the VI to rise from zero to the steady-state value, the VI is almost constant during the fault. The VI in this work is only designed to work with a certain range of grid impedance and bolted faults. Large variations in the grid impedance and the severity of the fault can affect the performance of this method [118].

Unlike the static VI, the value of the VI in [118] and [124] is set according to the amount of over-currents such that the output currents are restrained below an allowable level even in a three-phase bolted fault. In [118], a linear model of VI with respect to the output current is presented. The VI is activated when the output current exceeds a threshold value and varies linearly with the changes in the current. However, due to the interactions with parallel generators in the network, more complex nonlinear models of VI are required to precisely limit the output current. Apart from that, the method presented in [118] degrades if the grid impedance varies expeditiously. This scenario usually occurs due to line tripping and fault clearance. In [124], another linear model of VI is introduced. The VI is set proportionally to the difference between the over-current and a threshold value.

Apart from solely using VI, various voltage-based current limiters are also introduced in the literature. A current limiting solution combining both current saturator and VI is proposed in [122]. A fast current limiter scales down the current references' magnitude to keep the output currents below the limit. The voltage references are then subtracted by the virtual voltage drops to enhance the FRT process. Besides, Reference [128] introduces a nonlinear droop control with inherent current-limiting capability. The proposed control in [128] is developed by merging a virtual resistance design into the voltage droop control. However, due to the requirement of a PLL in this design, oscillations are observed in the inverter's responses. Moreover, this design decreases the inverter's fault current capability unnecessarily.

Additionally, in [129], a voltage-based current limiter is proposed without using the virtual resistor concept. Firstly, a theoretical relation between the maximum output current and the maximum output voltage of a GFMI is obtained. By limiting the output voltage below its maximum value calculated in the previous step, the output current is restrained. However, the role of the internal resistors of the LCL filter is not mentioned in defining the relation between the voltage and the current in this work. This potentially leads to inaccurate estimations of the maximum voltage value.

c: CURRENT LIMITING FOR ASYMMETRICAL FAULTS

Current limitation during asymmetrical faults varies depending on the reference frame. The natural reference frame (NARF), i.e., *abc*-frame, is the most preferable frame for dealing with asymmetrical faults. When an unbalanced fault occurs, the GFMI control is switched to a NARF to independently control each phase current of the

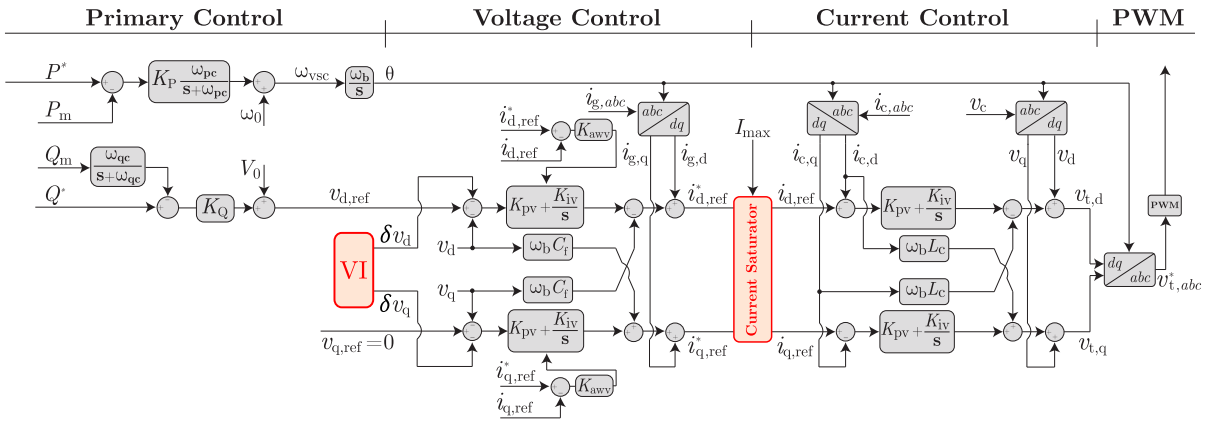

FIGURE 12. Implementations of the VI and the current saturator in a cascade grid forming control [111].

inverter [130]–[132]. However, this approach requires fault detection and independent control for each phase, hence increasing the complexity of the GFMI's control. Another approach for current limitation in the NARF is latching the current references of all three phases at a pre-defined waveform as mentioned in Section IV-C1 [114], [117], [133]. Nevertheless, applying the same current reference in all three phases during an asymmetrical fault can result in over-voltages and saturation of the pulse width modulation (PWM) in the healthy phases [114], [133]. To tackle these issues, parallel VI is first proposed in [114]. The design of the parallel VI is then detailed and analyzed in [133].

In addition, the stationary reference frame (STRF) is more preferable for asymmetrical faults, compared to the synchronous reference frame (SYRF) [122]. In the STRF, the current limitation should be designed with consideration for both positive- and negative-sequence currents to minimize the double-frequency harmonic and distortions [122]. Besides, in the SYRF, the current limiting methods aforementioned in Section IV-C1 can be extended for asymmetrical faults if a negative sequence control is added to the system [134].

2) FAULT RECOVERY OF GFMI

Fault recovery and large-signal transient stability of a GFMI depend on multiple aspects of the system, including the control structure and the over-current protection of the GFMI. In terms of the control structure, non-inertial and inertial control can result in different post-contingency behaviors. The analysis in [94] shows that the presence of inertia in the P-ω control loop might contribute to the system instability after a voltage sag event. However, studies on the impacts of the inertia on the recovery of the GFMI from a voltage disturbance are not discussed in [94]. Based on the analysis in [94], the authors of [135] conduct an analysis for the fault recovery of an inertial GFMI and propose an adaptive mode switching (AMS) method to tackle the positive-feedback in the active power control, which is observed in the inertial grid forming systems. The AMS detects occurrences of excessive overshoot in the power angle. If an excessive overshoot occurs, the sign of the gains in the power controller is flipped to prevent the power angle from exceeding the unstable equilibrium point.

In addition, the fault recovery process of a GFMI with either a current saturator or VI for current limitation is described in [111]. This work reveals that the VI offers a longer critical clearing time compared to the current saturator. This result aligns with the analysis in [119]. Besides, the critical clearing time can be extended by limiting the power-angle revolution during a fault. To slow down this revolution, the power references and the droop gain should be adjusted during a fault as detailed in [96] and [136], respectively.

Apart from that, oscillatory post-fault transients can degrade the recovery or even trigger protection devices in the network, leading to unnecessary disconnections of the GFMI. A series dynamic VI model, as shown in Fig. 13, can be integrated into the control in the fault recovery process to suppress the poor transients [96]. The VI is solely for transient enhancement, not for current limiting purposes as aforementioned. It is active only during the fault recovery process of the GFMI and disabled in the normal operation [96]. Additionally, a parallel VI model with the same function is also proposed in [117] to suppress post-fault voltage overshoots in microgrids.

V. APPLICATION OF GRID FORMING INVERTERS

A. APPLICATION OF GRID FORMING INVERTERS IN WEAK GRIDS

GFMIs can provide inertia, black start capability, frequency support, and voltage support for the weak grids with low-inertia [137]–[139]. The authors in [55] have proposed a method for designing VSG-based GFMI for the inductive and resistive weak grids. A small-signal model of the system for weak grid application is derived, and the robustness of the proposed method against the grid impedance variation

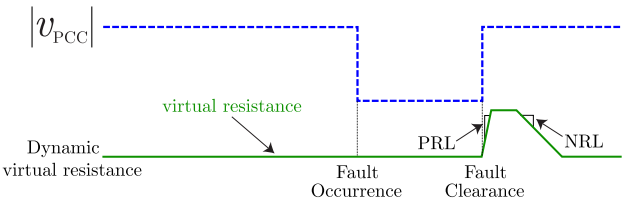

FIGURE 13. Dynamic virtual resistor for post-fault oscillation damping [96].

is examined. A virtual capacitor control loop is proposed in [130] to control a type-4 WT in a weak grid. The method is based on matching the inverter control system with the synchronous generator. The synchronous power control (SPC) accompanied by a novel current limiting method is suggested in [96] to control a GFMI in a weak grid.

The authors in [140] have studied the optimal placement of GFMIs and GFDIs in a low inertia power system for fast frequency response. The proposed optimization problem can optimize the controller parameters and the location of the device in the system to increase its resilience. The study also shows that the system robustness depends not only on the amount of virtual inertia used but also on the specific implementation and location of virtual inertia.

B. APPLICATION OF GRID FORMING INVERTERS IN HVDC CONVERTERS

Droop-based GFMI has been suggested for use in offshore AC networks with voltage source converter (VSC) based HVDC links [141], [142]. Small-signal stability analysis of the droop controller inverter, including cascade inner current-voltage loops, is derived in [141] for an offshore AC network. The block diagram of the mentioned system is shown in Fig. 14. The short circuit analysis of the same type of grid forming controller for an offshore network with multiple HVDC converters is studied in [143] and [144]. PSC controllers are proposed for VSC-HVDC applications, especially when connected to the weak grids, as the PSC gird-forming HVDCs can improve voltage stability in the weak grids [30]. Another grid forming control method to control the AC voltage and reduce the harmonics of the HVDC converters is proposed in [143]. The outer loop in this control method consists of an AC voltage controller and a DC-voltage controller to control the power-sharing in the system.

C. APPLICATION OF GFMI IN RENEWABLE ENERGY SOURCES

With the rapid increase of renewable energy generation in the last decades, the application of GFMI in both WTs and PV farms has received some attention in the literature.

1) APPLICATION OF GFMI IN WTs

Many VSG controllers have been proposed for various types of WTs [7]. Virtual synchronous control (VSynC) for a doubly-fed induction generator (DFIG) based WT is proposed in [144]. The block diagram of the VSynC controller is shown in Fig. 15. It uses a conventional swing equation-based VSG for the active power controller. Wind power in this method is considered a variable parameter consisting of two constant (pre-disturbance) and variation parts, which is different from most current works that consider wind power a constant parameter. The authors in [145] also propose VSynC grid forming controllers for a DFIG-based WT. Three operation areas are considered for the WT: MPPT area, maximal speed limit area, and the rated power area. In addition, pitch control is considered and based on the motion equation concept, the analysis of the inertia characteristic is derived.

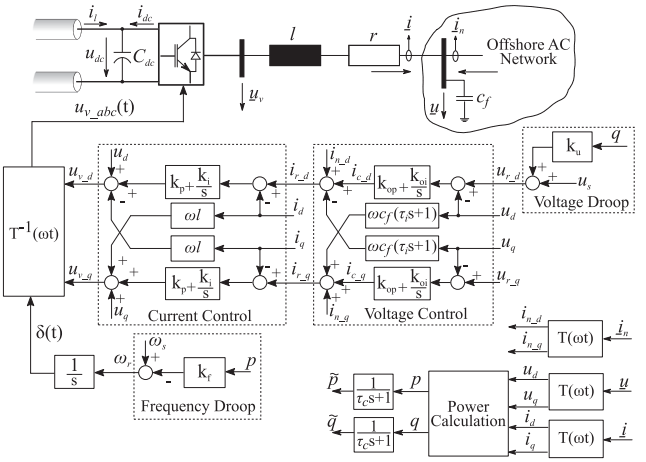

FIGURE 14. Grid forming HVDC system for an offshore AC network [141] *(Copyright © 2018, IEEE).*

Another VSG controller structure and its control principle for a WT is suggested in [146]. The controllers for the grid-side inverter, the machine-side inverter, the storage-side inverter, and the pitch part are explained. It considers three different modes for the WT: VSG with pitch control, VSG normal operation, and VSG with MPPT control. The transition between different operation modes and the sizing of the energy storage element are also discussed in [146]. The small-signal model of the system is derived, and also, to improve the stability of the system in the weak grids, a stabilization controller is proposed [146]. Another VSG-based grid forming control for DFIG-based wind farms to improve the stability of line-commutated converter (LCC) HVDC is proposed in [147]. The current control system, including the current limitation, is not mentioned in this study.

In [148], an SPC controller is used to control the active power at the grid-side inverter. They propose a system frequency response (SFR) model based on the motion equation concept to investigate the inertial dynamics of the WT. The equivalent inertia and the damping constant for the WT is calculated based on the proposed model. It should be mentioned that the wind speed variation, current control dynamics, and weak grid effects are not considered in this study. The authors in [149] indicated that as the VSG control method has cascade control loops, it can be challenging to tune the controllers in

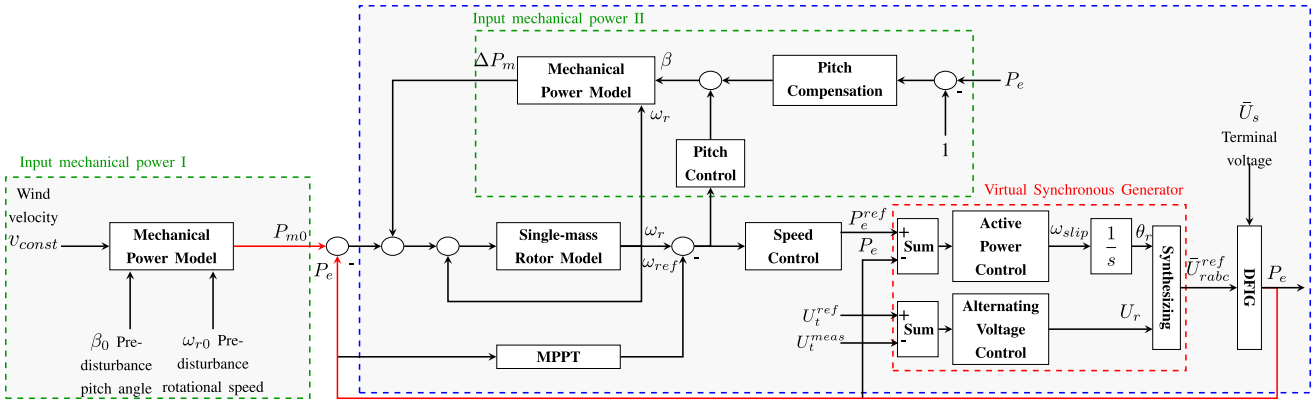

FIGURE 15. Control scheme for a DFIG-based WT with VSynC [144].

a decoupled way in low-frequency applications such as WTs. It instead proposes a virtual capacitor control loop based on matching the synchronous generator and the inverter.

2) APPLICATION OF GFMI IN SOLAR FARMS

Photovoltaic synchronous generator (PVSG) is proposed in [150]. In this method, an SPC grid forming control method for a supercapacitor-based inverter is utilized. The GFMI works in parallel with a traditional grid following PV plant, as is shown in Fig. 16, and by doing so, the whole system behaves as a PVSG that provides inertia to the system. It should be mentioned that this method needs more software and hardware for the grid forming system comparing to a conventional PV. It also requires the calculation of the sizing of the required supercapacitor. Last but not least, the GFMI needs to be physically implemented close to the GFLI to make sure the system works correctly, considering the impedance ratio between the inverters and PCC [150].

Another PV-based virtual synchronous generator is suggested in [151]. In this structure, a VSG based GFMI with variable inertia works in parallel with a PV plant. Based on the ω measurement, it proposes variable inertia constant in the VSG controller to improve the transient stability of the system. This study shows that the system with variable inertia has a better response compared to the constant inertia VSG and conventional PV, especially under weak solar irradiation. The work does not study the reactive power controller, current controller, and sizing of the energy storage system. Also, the system response has not been studied under fault and transient events [151]. Additionally, VSG control is used to synchronize the PV-inverter and the distributed generator (DG) without the usage of PLL and by correcting the DG rotor initial position in a standalone hybrid PV-diesel system in [152]. Virtual governor and virtual excitation voltage are modeled in this VSG controller, even though the current controller is not implemented in the control system. Another VSG grid forming control for PVs is proposed in [153]. A virtual step-out block is proposed and added to the VSG control system to improve the transient stability of the system.

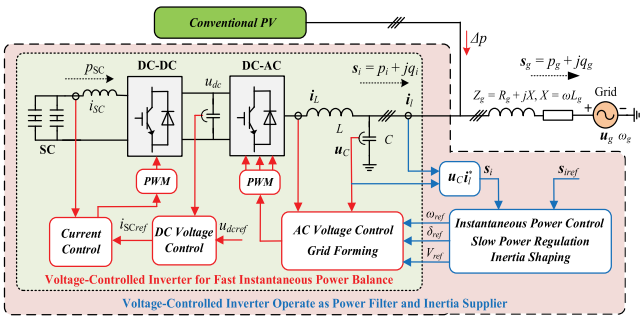

FIGURE 16. Schematic of the PVSG grid forming inverter [150] *(Copyright © 2020, IEEE)*.

Additionally, the necessity of a virtual governor system and the sizing of the energy storage system is discussed.

D. BLACK-START CAPABILITY OF GFMI

One unique advantage of GFMIs is the ability to provide black-start services in the event of wide-area blackouts with the help of renewable energy sources or battery energy storage. The authors in [154] investigate various GFMI control strategies implemented in HVDC-connected wind farms to energize onshore loads. Comparison of two energizing methods of black-start, i.e., hard switching and soft-start methods carried out in [155], indicates faster energization with smaller transients using soft-start. In [156], a direct voltage control based GFMI control of WT with black-start capability is proposed.

E. RECENT TRENDS IN GFMI IMPLEMENTATIONS

Dalrymple Battery Energy Storage System (BESS) - ABB: ElectraNet's 30 MW / 8 MWh, BESS at Dalrymple substation in South Australia, is a utility-scale implementation with GFMIs carried out by Hitachi ABB Power Grids. The Dalrymple BESS is the first large-scale grid forming BESS connected to the Australian National Electricity Market (NEM) and is built on Virtual Synchronous Generator technology, which strengthens the grid by replicating

the behavior and performance of a synchronous machine, providing synthetic inertia and high fault current to allow higher levels of renewable energy resources to connect and operate. The system also provides reliability and flexibility services such as fast power injection, seamless islanding and black-start of the local distribution network. When faults occur on the upstream feeder, the system seamlessly islands in co-ordination with the nearby 91 MW Wattle Point Wind Farm and distributed solar PV, to continue operating a local islanded power system to ensure continuity of supply to the local customers. This enables Dalrymple BESS to form one of the largest autonomous microgrids in the world during its islanded operation. The project's results and operation have demonstrated for the first time on the NEM the critical role GFMIs, as opposed to grid following inverters, can play in strengthening the grid and enabling high renewable targets to be met. In addition to this, the Dalrymple BESS offers competitive market services to the NEM, providing a commercial return to the operator, which isn't possible currently with comparable power system support technology such as synchronous condensers. [157], [158].

Hornsdale BESS - Tesla: The 150 MW / 193.5 MWh power reserve located in Jamestown, South Australia, is situated next to the 315 MW Hornsdale wind farm. The battery has already shown its immense value for the grid in a number of ways, largely through grid stabilization services and savings [159]. The pre-existing grid following control has recently been updated to grid forming control through a software update [160].

Alinta Energy BESS - ABB: Alinta Energy's BESS implemented by ABB interfaced through a 30 MW VSG provides a spinning reserve for off-grid mining operations in Newman, Western Australia. The BESS is also capable of energizing long capacitive lines and black-starting the mine [158].

General Electric: GE has had multiple implementations of GFMI that are tailor-made for specific applications. The 30 MW / 22 MWh BESS at Imperial Ignition District, California, is used for black-starting a gas turbine. Another recent implementation is located at the Perryville generating station with a rating of 7.4MW / 6.6 MWh, commissioned in 2019. Recently, GE research secured 4.2 million dollars funding from U.S. Department of Energy Solar Energy Technologies Office (SETO) to develop grid forming solar inverter control technologies [161]. GE aims to develop grid forming controls to allow wind and solar inverters to improve the transient stability of systems with high renewable energy resources penetration.

Dersalloch Windfarm - National Grid UK, Scottish Power Renewables: The 69 MW farms with 23 units of Siemens Gemesa Turbines is the first large-scale implementation of GFMI control by a wind farm. The project is commissioned, and the black-start capability was demonstrated in November 2020 [162]. The wind farm is able to regulate the local frequency and voltage, forming a stable network island before connecting to the rest of the grid.

AusNet Services GESS: The Grid Energy Storage Systems (GESS) commissioned by ABB in 2014 consists of a 1 MWh 1C lithium battery system that interfaces to the microgrid through a 1 MVA VSG inverters and a 1 MVA diesel generator connected to the grid through a 3 MVA three-winding transformer. The system is located at an end-of-line distribution feeder in an industrial estate situated in the northern suburbs of Melbourne. AusNet Services aimed to test a non-network option to manage peak demand with the potential to defer network augmentation, and GESS proved to be a suitable candidate. It is demonstrated that such an embedded generation source can also provide peak load support by reducing the upstream feeder requirements during peak consumption periods by supplying the loads locally. Given the capabilities of the GESS with regards to power system quality, AusNet Services also planned to investigate the effect on local system quality and stability that the GESS provides, such as power factor, voltage support, harmonics, flicker, and negative sequence voltage. Additionally, the islanding capabilities of the GESS have been investigated by AusNet Services to improve system supply and stability in the case of larger network faults. In the event of a fault, the GESS islands the downstream feeder, creating an islanded microgrid which the GESS would supply until its energy reserves are depleted, or the fault is cleared. When the fault is cleared, the GESS would reconnect to the grid and transfer the supply back to the network and begin recharging the batteries on a scheduled, preset programmed time of day [163].

VI. RESEARCH DIRECTIONS

A. FREQUENCY CONTROL

From the above discussions, it is clearly evident that traditional frequency control approaches have to be revisited as the share of IBRs increase in AC power systems. For GFMIs to be considered as a promising solution, the two fundamental research questions that have to be answered are: 1) can GFMIs achieve frequency regulation in heterogeneous systems comprising GFLIs and synchronous generators?, and 2) are there any limitations on the share of GFMIs in power systems? [1]. Moreover, along with the development of IBRs, another operational level question that would arise is how important it is to regulate frequency and would the frequency tolerance band and RoCoF limits can be relaxed, especially in fully inverter-based power grids. The generation source for GFMIs is mostly wind and solar, where frequency control pushes them to operate in non-optimal regions. In certain situations, the extracted power might not be sufficient to meet the requirement. Energy storage is a promising solution to this issue. Nevertheless, determining the suitable type of energy storage and optimal capacity to keep the frequency within acceptable limits are open research questions in relation to GFMIs. The other operational concern to be addressed is the proper load sharing mechanism between grid forming assets available in the system and whether traditional droop-based techniques are

still useful, or a proper communication mechanism is needed to manage the frequency control and load sharing between isochronously-controlled grid forming assets.

B. VOLTAGE REGULATION

With the increase of GFMIs and GFLIs, the volt/VAR control shifts from large synchronous generators to distributed generation sources. Therefore, it is important to understand how these distributed, and local volt/VAR controls affect the voltage regulation in the entire power system. Moreover, the impact on the exciter control of Syncons and GFMIs should be investigated. Finding the locations of GFMIs to obtain optimal voltage regulation results is another important research area related to GFMIs. Moreover, the suitability of traditional QV droop control and the necessity of communication-based volt/VAR control are to be investigated, especially at increased penetration of GFMIs and GFLIs.

C. SYSTEM STRENGTH

Even though VSG as an advanced form of GFMIs demonstrated its merit in effectively contributing to the system strength of high renewable-penetrated networks, the role of each VSG components such as virtual inertia, synthetic impedance, damper winding's, and flux model or their combined effect has not been fully worked out yet. Clarifying this can lead to identifying key players of the system strength enhancement and help with the improvement of stability through the allocation of sufficient factor.

D. REGULATORY FRAMEWORK

The implementation of GFMIs require demonstration of the above-mentioned key functionalities, mainly frequency and voltage regulation, and developing confidence among the grid operators and regulators. Since GFMI is relatively a new technology, grid integration should take a gradual approach where its frequency and voltage regulation capabilities should be demonstrated in microgrids at early stages [1]. Adding GFMIs into larger power systems should take place at gradually increasing power levels. Moreover, it is essential to establish technical standards, commissioning procedures and amend other relevant regulatory frameworks to reflect capabilities and limitations of GFMIs, especially fault ride-through and fault current levels.

VII. CONCLUSION

GFMIs have emerged as a promising solution for the issues related to the high penetration of IBRs and weak grid scenarios. While having successful implementations in Australia, the US, and the UK at various power levels, the widespread use of GFMIs requires further advancements in their technologies and regulatory acceptance. This paper identifies several key challenges related to GFMIs, including small-signal stability, transient stability, over-current protection, and seamless transition between grid-connected and standalone modes. Moreover, control methodologies proposed in the literature for GFMIs are critically reviewed. The conceptual differences between GFMIs and GFLIs are also discussed, highlighting the need for grid support, especially for weaker parts of the grid. The areas which require further research and development are also identified and commented on. In addition to the technological developments, regulatory support and acceptance are key enablers for successful implementations of GFMIs in large power grids.

REFERENCES

[1] Y. Lin, J. H. Eto, B. B. Johnson, J. D. Flicker, R. H. Lasseter, H. N. V. Pico, G.-S. Seo, B. J. Pierre, and A. Ellis, "Research roadmap on grid-forming inverters," Nat. Renew. Energy Lab., Golden, CO, USA, Tech. Rep. NREL/TP-5D00-73476, 2020.
[2] H. Han, X. Hou, J. Yang, J. Wu, M. Su, and J. M. Guerrero, "Review of power sharing control strategies for islanding operation of AC microgrids," *IEEE Trans. Smart Grid*, vol. 7, no. 1, pp. 200–215, Jan. 2016.
[3] T. L. Vandoorn, J. D. M. De Kooning, B. Meersman, and Y. L. Vandevelde, "Review of primary control strategies for islanded microgrids with power-electronic interfaces," *Renew. Sustain. Energy Rev.*, vol. 19, pp. 613–628, Mar. 2013. [Online]. Available: http://www.sciencedirect.com/science/article/pii/S1364032112006764
[4] J. Liu, Y. Miura, H. Bevrani, and T. Ise, "Enhanced virtual synchronous generator control for parallel inverters in microgrids," *IEEE Trans. Smart Grid*, vol. 8, no. 5, pp. 2268–2277, Sep. 2017.
[5] H. Bevrani, T. Ise, and Y. Miura, "Virtual synchronous generators: A survey and new perspectives," *Int. J. Electr. Power Energy Syst.*, vol. 54, pp. 244–254, Jan. 2014.
[6] U. Tamrakar, D. Shrestha, M. Maharjan, B. P. Bhattarai, T. M. Hansen, and R. Tonkoski, "Virtual inertia: Current trends and future directions," *Appl. Sci.*, vol. 7, no. 7, p. 654, 2017.
[7] L. Lu and N. A. Cutululis, "Virtual synchronous machine control for wind turbines: A review," *J. Phys., Conf. Ser.*, vol. 1356, Oct. 2019, Art. no. 012028.
[8] P. Unruh, M. Nuschke, P. Strauß, and F. Welck, "Overview on grid-forming inverter control methods," *Energies*, vol. 13, no. 10, p. 2589, May 2020.
[9] R. Rosso, X. Wang, M. Liserre, X. Lu, and S. Engelken, "Grid-forming converters: An overview of control approaches and future trends," in *Proc. IEEE Energy Convers. Congr. Expo. (ECCE)*, Oct. 2020, pp. 4292–4299.
[10] R. Rosso, X. Wang, M. Liserre, X. Lu, and S. Engelken, "Grid-forming converters: Control approaches, grid-synchronization, and future trends—A review," *IEEE Open J. Ind. Appl.*, vol. 2, pp. 93–109, 2021.
[11] K. S. Ratnam, K. Palanisamy, and G. Yang, "Future low-inertia power systems: Requirements, issues, and solutions—A review," *Renew. Sustain. Energy Rev.*, vol. 124, May 2020, Art. no. 109773. [Online]. Available: https://www.sciencedirect.com/science/article/pii/S1364032120300691
[12] B. Mirafzal and A. Adib, "On grid-interactive smart inverters: Features and advancements," *IEEE Access*, vol. 8, pp. 160526–160536, 2020.
[13] D. Pattabiraman, R. H. Lasseter, and T. M. Jahns, "Comparison of grid following and grid forming control for a high inverter penetration power system," in *Proc. IEEE Power Energy Soc. Gen. Meeting (PESGM)*, Aug. 2018, pp. 1–5.
[14] J. Matevosyan, B. Badrzadeh, T. Prevost, E. Quitmann, D. Ramasubramanian, H. Urdal, S. Achilles, J. MacDowell, S. H. Huang, V. Vital, and J. O'Sullivan, "Grid-forming inverters: Are they the key for high renewable penetration?" *IEEE Power Energy Mag.*, vol. 17, no. 6, pp. 89–98, Nov./Dec. 2019.
[15] J. Rocabert, A. Luna, F. Blaabjerg, and P. Rodriguez, "Control of power converters in AC microgrids," *IEEE Trans. Power Electron.*, vol. 27, no. 11, pp. 4734–4749, Nov. 2012.
[16] E. A. A. Coelho, P. C. Cortizo, and P. F. D. Garcia, "Small signal stability for single phase inverter connected to stiff AC system," in *Proc. Conf. Rec. IEEE Ind. Appl. Conf. 34th IAS Annu. Meeting*, vol. 4, Oct. 1999, pp. 2180–2187.
[17] X. Guo, Z. Lu, B. Wang, X. Sun, L. Wang, and J. M. Guerrero, "Dynamic phasors-based modeling and stability analysis of droop-controlled inverters for microgrid applications," *IEEE Trans. Smart Grid*, vol. 5, no. 6, pp. 2980–2987, Nov. 2014.

[18] B. Mahamedi and J. E. Fletcher, "The equivalent models of grid-forming inverters in the sequence domain for the steady-state analysis of power systems," *IEEE Trans. Power Syst.*, vol. 35, no. 4, pp. 2876–2887, Jul. 2020.

[19] W. Du, F. Tuffner, K. P. Schneider, R. H. Lasseter, J. Xie, Z. Chen, and B. P. Bhattarai, "Modeling of grid-forming and grid-following inverters for dynamic simulation of large-scale distribution systems," *IEEE Trans. Power Delivery*, vol. 36, no. 4, pp. 2035–2045, Aug. 2020.

[20] K. V. Kkuni, S. Mohan, G. Yang, and W. Xu, "Comparative assessment of typical controlrealizations of grid forming converters based ontheir voltage source behaviour," 2021, *arXiv:2106.10048*. [Online]. Available: https://arxiv.org/abs/2106.10048

[21] M. C. Chandorkar, D. M. Divan, and R. Adapa, "Control of parallel connected inverters in standalone AC supply systems," *IEEE Trans. Ind. Appl.*, vol. 29, no. 1, pp. 136–143, Jan./Feb. 1993.

[22] N. Pogaku, M. Prodanovic, and T. C. Green, "Modeling, analysis and testing of autonomous operation of an inverter-based microgrid," *IEEE Trans. Power Electron.*, vol. 22, no. 2, pp. 613–625, Mar. 2007.

[23] J. M. Guerrero, L. G. Vicuna, J. Matas, M. Castilla, and J. Miret, "A wireless controller to enhance dynamic performance of parallel inverters in distributed generation systems," *IEEE Trans. Power Electron.*, vol. 19, no. 5, pp. 1205–1213, Sep. 2004.

[24] K. De Brabandere, B. Bolsens, J. Van den Keybus, A. Woyte, J. Driesen, and R. Belmans, "A voltage and frequency droop control method for parallel inverters," *IEEE Trans. Power Electron.*, vol. 22, no. 4, pp. 1107–1115, Jul. 2007.

[25] J. M. Guerrero, L. G. de Vicuna, J. Matas, M. Castilla, and J. Miret, "Output impedance design of parallel-connected UPS inverters with wireless load-sharing control," *IEEE Trans. Ind. Electron.*, vol. 52, no. 4, pp. 1126–1135, Aug. 2005.

[26] L. Huang, H. Xin, and F. Dörfler, "H_∞-control of grid-connected converters: Design, objectives and decentralized stability certificates," *IEEE Trans. Smart Grid*, vol. 11, no. 5, pp. 3805–3816, Sep. 2020.

[27] R. K. Sharma, S. Mishra, and D. Pullaguram, "A robust $\mathcal{H}_\infty$ multivariable stabilizer design for droop based autonomous AC microgrid," *IEEE Trans. Power Syst.*, vol. 35, no. 6, pp. 4369–4382, Jun. 2020.

[28] R. Majumder, B. Chaudhuri, A. Ghosh, R. Majumder, G. Ledwich, and F. Zare, "Improvement of stability and load sharing in an autonomous microgrid using supplementary droop control loop," *IEEE Trans. Power Syst.*, vol. 25, no. 2, pp. 796–808, May 2010.

[29] J. Hu, J. Zhu, D. G. Dorrell, and J. M. Guerrero, "Virtual flux droop method—A new control strategy of inverters in microgrids," *IEEE Trans. Power Electron.*, vol. 29, no. 9, pp. 4704–4711, Sep. 2014.

[30] L. Zhang, L. Harnefors, and H.-P. Nee, "Power-synchronization control of grid-connected voltage-source converters," *IEEE Trans. Power Syst.*, vol. 25, no. 2, pp. 809–820, May 2010.

[31] L. Harnefors, M. Hinkkanen, U. Riaz, F. M. M. Rahman, and L. Zhang, "Robust analytic design of power-synchronization control," *IEEE Trans. Ind. Electron.*, vol. 66, no. 8, pp. 5810–5819, Aug. 2019.

[32] H.-P. Beck and R. Hesse, "Virtual synchronous machine," in *Proc. 9th Int. Conf. Electr. Power Qual. Utilisation*, Oct. 2007, pp. 1–6.

[33] Y. Chen, R. Hesse, D. Turschner, and H. Beck, "Comparison of methods for implementing virtual synchronous machine on inverters," in *Proc. Int. Conf. Renew. Energies Power Qual. (ICREPQ)*, 2012, pp. 1–6.

[34] J. Driesen and K. Visscher, "Virtual synchronous generators," in *Proc. IEEE Power Energy Soc. Gen. Meeting-Convers. Del. Electr. Energy 21st Century*, Jul. 2008, pp. 1–3.

[35] M. Guan, W. Pan, J. Zhang, Q. Hao, J. Cheng, and X. Zheng, "Synchronous generator emulation control strategy for voltage source converter (VSC) stations," *IEEE Trans. Power Syst.*, vol. 30, no. 6, pp. 3093–3101, Nov. 2015.

[36] S. D'Arco and J. A. Suul, "Equivalence of virtual synchronous machines and frequency-droops for converter-based microgrids," *IEEE Trans. Smart Grid*, vol. 5, no. 1, pp. 394–395, Jan. 2014.

[37] J. Liu, Y. Miura, and T. Ise, "Comparison of dynamic characteristics between virtual synchronous generator and droop control in inverter-based distributed generators," *IEEE Trans. Power Electron.*, vol. 31, no. 5, pp. 3600–3611, May 2016.

[38] J. Alipoor, Y. Miura, and T. Ise, "Power system stabilization using virtual synchronous generator with alternating moment of inertia," *IEEE J. Emerg. Sel. Topics Power Electron.*, vol. 3, no. 2, pp. 451–458, Jun. 2015.

[39] M. A. L. Torres, L. A. C. Lopes, L. A. T. Morán, and J. R. C. Espinoza, "Self-tuning virtual synchronous machine: A control strategy for energy storage systems to support dynamic frequency control," *IEEE Trans. Energy Convers.*, vol. 29, no. 4, pp. 833–840, Dec. 2014.

[40] D. Li, Q. Zhu, S. Lin, and X. Y. Bian, "A self-adaptive inertia and damping combination control of VSG to support frequency stability," *IEEE Trans. Energy Convers.*, vol. 32, no. 1, pp. 397–398, Mar. 2017.

[41] F. Wang, L. Zhang, X. Feng, and H. Guo, "An adaptive control strategy for virtual synchronous generator," *IEEE Trans. Ind Appl.*, vol. 54, no. 5, pp. 5124–5133, Sep./Oct. 2018.

[42] M. P. N. van Wesenbeeck, S. W. H. de Haan, P. Varela, and K. Visscher, "Grid tied converter with virtual kinetic storage," in *Proc. IEEE Bucharest PowerTech*, Jun. 2009, pp. 1–7.

[43] W. Zhang, A. M. Cantarellas, J. Rocabert, A. Luna, and P. Rodriguez, "Synchronous power controller with flexible droop characteristics for renewable power generation systems," *IEEE Trans. Sust. Energy*, vol. 7, no. 4, pp. 1572–1582, Oct. 2016.

[44] W. Zhang, A. Tarraso, J. Rocabert, A. Luna, J. I. Candela, and P. Rodriguez, "Frequency support properties of the synchronous power control for grid-connected converters," *IEEE Trans. Ind. Appl.*, vol. 55, no. 5, pp. 5178–5189, Sep. 2019.

[45] X. Quan, A. Q. Huang, and H. Yu, "A novel order reduced synchronous power control for grid-forming inverters," *IEEE Trans. Ind. Electron.*, vol. 67, no. 12, pp. 10989–10995, Dec. 2020.

[46] X. Meng, J. Liu, and Z. Liu, "A generalized droop control for grid-supporting inverter based on comparison between traditional droop control and virtual synchronous generator control," *IEEE Trans. Power Electron.*, vol. 34, no. 6, pp. 5416–5438, Jun. 2019.

[47] G. N. Baltas, N. B. Lai, L. Marin, A. Tarrasó, and P. Rodriguez, "Grid-forming power converters tuned through artificial intelligence to damp subsynchronous interactions in electrical grids," *IEEE Access*, vol. 8, pp. 93369–93379, 2020.

[48] T. Qoria, E. Rokrok, A. Bruyere, B. François, and X. Guillaud, "A PLL-free grid-forming control with decoupled functionalities for high-power transmission system applications," *IEEE Access*, vol. 8, pp. 197363–197378, 2020.

[49] A. Karimi, Y. Khayat, M. Naderi, T. Dragicevic, R. Mirzaei, F. Blaabjerg, and H. Bevrani, "Inertia response improvement in AC microgrids: A fuzzy-based virtual synchronous generator control," *IEEE Trans. Power Electron.*, vol. 35, no. 4, pp. 4321–4331, Apr. 2020.

[50] Q.-C. Zhong and G. Weiss, "Synchronverters: Inverters that mimic synchronous generators," *IEEE Trans. Ind. Electron.*, vol. 58, no. 4, pp. 1259–1267, Apr. 2011.

[51] Q.-C. Zhong, P.-L. Nguyen, Z. Ma, and W. Sheng, "Self-synchronized synchronverters: Inverters without a dedicated synchronization unit," *IEEE Trans. Power Electron.*, vol. 29, no. 2, pp. 617–630, Feb. 2014.

[52] X. Wang, L. Chen, D. Sun, L. Zhang, and H. Nian, "A modified self-synchronized synchronverter in unbalanced power grids with balanced currents and restrained power ripples," *Energies*, vol. 12, no. 5, p. 923, Mar. 2019, doi: 10.3390/en12050923.

[53] S. Dong and Y. C. Chen, "Adjusting synchronverter dynamic response speed via damping correction loop," *IEEE Trans. Energy Convers.*, vol. 32, no. 2, pp. 608–619, Jun. 2017.

[54] S. Dong and Y. C. Chen, "A method to directly compute synchronverter parameters for desired dynamic response," *IEEE Trans. Energy Convers.*, vol. 33, no. 2, pp. 814–825, Jun. 2018.

[55] J. Roldán-Pérez, A. Rodríguez-Cabero, and M. Prodanovic, "Design and analysis of virtual synchronous machines in inductive and resistive weak grids," *IEEE Trans. Energy Convers.*, vol. 34, no. 4, pp. 1818–1828, Dec. 2019.

[56] T. Jouini, C. Arghir, and F. Dörfler, "Grid-friendly matching of synchronous machines by tapping into the DC storage," *IFAC-PapersOnLine*, vol. 49, no. 22, pp. 192–197, 2016. [Online]. Available: http://www.sciencedirect.com/science/article/pii/S2405896316319826

[57] C. Arghir, T. Jouini, and F. Dörfler, "Grid-forming control for power converters based on matching of synchronous machines," *Automatica*, vol. 95, pp. 273–282, Sep. 2018.

[58] C. Arghir and F. Dörfler, "The electronic realization of synchronous machines: Model matching, angle tracking, and energy shaping techniques," *IEEE Trans. Power Electron.*, vol. 35, no. 4, pp. 4398–4410, Apr. 2020.

[59] B. B. Johnson, S. V. Dhople, A. O. Hamadeh, and P. T. Krein, "Synchronization of parallel single-phase inverters with virtual oscillator control," *IEEE Trans. Power Electron.*, vol. 29, no. 11, pp. 6124–6138, Dec. 2014.

[60] B. B. Johnson, S. V. Dhople, J. L. Cale, A. O. Hamadeh, and P. T. Krein, "Oscillator-based inverter control for islanded three-phase microgrids," *IEEE J. Photovolt.*, vol. 4, no. 1, pp. 387–395, Jan. 2014.
[61] B. B. Johnson, M. Sinha, N. G. Ainsworth, F. Dörfler, and S. V. Dhople, "Synthesizing virtual oscillators to control islanded inverters," *IEEE Trans. Power Electron.*, vol. 31, no. 8, pp. 6002–6015, Aug. 2016.
[62] M. Sinha, F. Dörfler, B. B. Johnson, and S. V. Dhople, "Uncovering droop control laws embedded within the nonlinear dynamics of van der pol oscillators," *IEEE Trans. Control Netw. Syst.*, vol. 4, no. 2, pp. 347–358, Jun. 2017.
[63] M. Colombino, D. Groß, and F. Dörfler, "Global phase and voltage synchronization for power inverters: A decentralized consensus-inspired approach," in *Proc. IEEE 56th Annu. Conf. Decis. Control (CDC)*, Dec. 2017, pp. 5690–5695.
[64] M. Colombino, D. Groß, J. Brouillon, and F. Dörfler, "Global phase and magnitude synchronization of coupled oscillators with application to the control of grid-forming power inverters," *IEEE Trans. Autom. Control*, vol. 64, no. 11, pp. 4496–4511, Nov. 2019.
[65] D. Groß, M. Colombino, J. Brouillon, and F. Dörfler, "The effect of transmission-line dynamics on grid-forming dispatchable virtual oscillator control," *IEEE Trans. Control Netw. Syst.*, vol. 6, no. 3, pp. 1148–1160, Sep. 2019.
[66] M. A. Awal, H. Yu, H. Tu, S. M. Lukic, and I. Husain, "Hierarchical control for virtual oscillator based grid-connected and islanded microgrids," *IEEE Trans. Power Electron.*, vol. 35, no. 1, pp. 988–1001, Jan. 2020.
[67] M. A. Awal, H. Yu, I. Husain, W. Yu, and S. M. Lukic, "Selective harmonic current rejection for virtual oscillator controlled grid-forming voltage source converters," *IEEE Trans. Power Electron.*, vol. 35, no. 8, pp. 8805–8818, Aug. 2020.
[68] M. A. Awal and I. Husain, "Unified virtual oscillator control for grid-forming and grid-following converters," *IEEE J. Emerg. Sel. Topics Power Electron.*, vol. 9, no. 4, pp. 4573–4586, Aug. 2021.
[69] C. Kammer and A. Karimi, "Decentralized and distributed transient control for microgrids," *IEEE Trans. Control Syst. Technol.*, vol. 27, no. 1, pp. 311–322, Jan. 2019.
[70] S. S. Madani, C. Kammer, and A. Karimi, "Data-driven distributed combined primary and secondary control in microgrids," *IEEE Trans. Control Syst. Technol.*, vol. 29, no. 3, pp. 1340–1347, May 2021.
[71] L. Huang, H. Xin, Z. Wang, K. Wu, H. Wang, J. Hu, and C. Lu, "A virtual synchronous control for voltage-source converters utilizing dynamics of DC-link capacitor to realize self-synchronization," *IEEE J. Emerg. Sel. Topics Power Electron.*, vol. 5, no. 4, pp. 1565–1577, Dec. 2017.
[72] Y. Jiang, A. Bernstein, P. Vorobev, and E. Mallada, "Grid-forming frequency shaping control for low-inertia power systems," *IEEE Control Syst. Lett.*, vol. 5, no. 6, pp. 1988–1993, Dec. 2021.
[73] W. Du, Z. Chen, K. P. Schneider, R. H. Lasseter, S. P. Nandanoori, F. K. Tuffner, and S. Kundu, "A comparative study of two widely used grid-forming droop controls on microgrid small-signal stability," *IEEE J. Emerg. Sel. Topics Power Electron.*, vol. 8, no. 2, pp. 963–975, Jun. 2020.
[74] U. Markovic, O. Stanojev, P. Aristidou, E. Vrettos, D. S. Callaway, and G. Hug, "Understanding small-signal stability of low-inertia systems," *IEEE Trans. Power Syst.*, early access, Feb. 23, 2021, doi: 10.1109/TPWRS.2021.3061434.
[75] L. Ding, Y. Men, Y. Du, X. Lu, B. Chen, J. Tan, and Y. Lin, "Region-based stability analysis of resilient distribution systems with hybrid grid-forming and grid-following inverters," in *Proc. IEEE Energy Convers. Congr. Expo. (ECCE)*, Oct. 2020, pp. 3733–3740.
[76] R. Rosso, J. Cassoli, G. Buticchi, S. Engelken, and M. Liserre, "Robust stability analysis of LCL filter based synchronverter under different grid conditions," *IEEE Trans. Power Electron.*, vol. 34, no. 6, pp. 5842–5853, Jun. 2019.
[77] R. Rosso, S. Engelken, and M. Liserre, "Robust stability analysis of synchronverters operating in parallel," *IEEE Trans. Power Electron.*, vol. 34, no. 1, pp. 11309–11319, Nov. 2019.
[78] R. Rosso, S. Engelken, and M. Liserre, "Robust stability investigation of the interactions among grid-forming and grid-following converters," *IEEE J. Emerg. Sel. Topics Power Electron.*, vol. 8, no. 2, pp. 991–1003, Jun. 2020.
[79] Y. Qi, H. Deng, J. Wang, and Y. Tang, "Passivity-based synchronization stability analysis for power-electronic-interfaced distributed generations," *IEEE Trans. Sustain. Energy*, vol. 12, no. 2, pp. 1141–1150, Apr. 2020.
[80] Y. Peng, Y. Wang, Y. Liu, P. Yu, S. Shu, and W. Lei, "A full sequence impedance modelling and stability analysis of the virtual synchronous generator with inner loops," *IET Renew Power Gener.*, vol. 15, pp. 397–408, Feb. 2021.
[81] C. Li, J. Liang, L. M. Cipcigan, W. Ming, F. Colas, and X. Guillaud, "DQ impedance stability analysis for the power-controlled grid-connected inverter," *IEEE Trans. Energy Convers.*, vol. 35, no. 4, pp. 1762–1771, May 2020.
[82] C. Yang, L. Huang, H. Xin, and P. Ju, "Placing grid-forming converters to enhance small signal stability of PLL-integrated power systems," *IEEE Trans. Power Syst.*, vol. 36, no. 4, pp. 3563–3573, Jul. 2020.
[83] W. Dong, H. Xin, D. Wu, and L. Huang, "Small signal stability analysis of multi-infeed power electronic systems based on grid strength assessment," *IEEE Trans. Power Syst.*, vol. 34, no. 2, pp. 1393–1403, Mar. 2019.
[84] A. Crivellaro, A. Tayyebi, C. Gavriluta, D. Groß, A. Anta, F. Kupzog, and F. Dörfler, "Beyond low-inertia systems: Massive integration of grid-forming power converters in transmission grids," in *Proc. IEEE Power Energy Soc. General Meeting*, Aug. 2019, pp. 1–5.
[85] A. Tayyebi, D. Groß, A. Anta, F. Kupzog, and F. Dörfler, "Interactions of grid-forming power converters and synchronous machines," 2019, *arXiv:1902.10750*. [Online]. Available: https://arxiv.org/abs/1902.10750
[86] A. Tayyebi, D. Groß, A. Anta, F. Kupzog, and F. Dörfler, "Frequency stability of synchronous machines and grid-forming power converters," *IEEE J. Emerg. Sel. Topics Power Electron.*, vol. 8, no. 2, pp. 1004–1018, Jun. 2020.
[87] T. Liu and X. Wang, "Transient stability of single-loop voltage-magnitude controlled grid-forming converters," *IEEE Trans. Power Electron.*, vol. 36, no. 6, pp. 6158–6162, Jun. 2021.
[88] H. Xin, L. Huang, L. Zhang, Z. Wang, and J. Hu, "Synchronous instability mechanism of P-f droop-controlled voltage source converter caused by current saturation," *IEEE Trans. Power Syst.*, vol. 31, no. 6, pp. 5206–5207, Nov. 2016.
[89] C. Li, Y. Yang, Y. Cao, L. Wang, and F. Blaabjerg, "Frequency and voltage stability analysis of grid-forming virtual synchronous generator attached to weak grid," *IEEE J. Emerg. Sel. Topics Power Electron.*, early access, Dec. 2, 2021, doi: 10.1109/JESTPE.2020.3041698.
[90] X. Fu, J. Sun, M. Huang, Z. Tian, H. Yan, H. H.-C. Iu, P. Hu, and X. Zha, "Large-signal stability of grid-forming and grid-following controls in voltage source converter: A comparative study," *IEEE Trans. Power Electron.*, vol. 36, no. 7, pp. 7832–7840, Jul. 2021.
[91] Z. Shuai, C. Shen, X. Liu, Z. Li, and Z. J. Shen, "Transient angle stability of virtual synchronous generators using Lyapunov's direct method," *IEEE Trans. Smart Grid*, vol. 10, no. 4, pp. 4648–4661, Jul. 2018.
[92] M. Eskandari and A. V. Savkin, "On the impact of fault ride-through on transient stability of autonomous microgrids: Nonlinear analysis and solution," *IEEE Trans. Smart Grid*, vol. 12, no. 2, pp. 999–1010, Mar. 2021.
[93] H. Wu and X. Wang, "Design-oriented transient stability analysis of grid-connected converters with power synchronization control," *IEEE Trans. Ind. Electron.*, vol. 66, no. 8, pp. 6473–6482, Aug. 2019.
[94] D. Pan, X. Wang, F. Liu, and R. Shi, "Transient stability of voltage-source converters with grid-forming control: A design-oriented study," *IEEE J. Emerg. Sel. Topics Power Electron.*, vol. 8, no. 2, pp. 1019–1033, Jun. 2020.
[95] M. A. Awal and I. Husain, "Transient stability assessment for current constrained and unconstrained fault ride-through in virtual oscillator controlled converters," *IEEE Trans. Emerg. Sel. Topics Power Electron.*, early access, May 13, 2021, doi: 10.1109/JESTPE.2021.3080236.
[96] M. G. Taul, X. Wang, P. Davari, and F. Blaabjerg, "Current limiting control with enhanced dynamics of grid-forming converters during fault conditions," *IEEE Trans. Emerg. Sel. Topics Power Electron.*, vol. 8, no. 2, pp. 1062–1073, Jun. 2020.
[97] Z. Shuai, W. Huang, Z. J. Shen, A. Luo, and Z. Tian, "Active power oscillation and suppression techniques between two parallel synchronverters during load fluctuations," *IEEE Trans. Power Electron.*, vol. 35, no. 4, pp. 4127–4142, Apr. 2020.
[98] X. Xiong, C. Wu, B. Hu, D. Pan, and F. Blaabjerg, "Transient damping method for improving the synchronization stability of virtual synchronous generators," *IEEE Trans. Power Electron.*, vol. 36, no. 7, pp. 7820–7831, Jul. 2021.

[99] H. Yu, M. A. Awal, H. Tu, I. Husain, and S. Lukic, "Comparative transient stability assessment of droop and dispatchable virtual oscillator controlled grid-connected inverters," *IEEE Trans. Power Electron.*, vol. 36, no. 2, pp. 2119–2130, Feb. 2021.

[100] C. Shen, Z. Shuai, Y. Shen, Y. Peng, X. Liu, Z. Li, and Z. J. Shen, "Transient stability and current injection design of paralleled current-controlled VSCs and virtual synchronous generators," *IEEE Trans. Smart Grid*, vol. 12, no. 2, pp. 1118–1134, Mar. 2021.

[101] H. Cheng, Z. Shuai, C. Shen, X. Liu, Z. Li, and Z. J. Shen, "Transient angle stability of paralleled synchronous and virtual synchronous generators in islanded microgrids," *IEEE Trans. Power Electron.*, vol. 35, no. 8, pp. 8751–8765, Aug. 2020.

[102] M. N. Arafat, S. Palle, Y. Sozer, and I. Husain, "Transition control strategy between standalone and grid-connected operations of voltage-source inverters," *IEEE Trans. Ind. Appl.*, vol. 48, no. 5, pp. 1516–1525, Sep. 2012.

[103] T.-V. Tran, T.-W. Chun, H.-H. Lee, H.-G. Kim, and E.-C. Nho, "PLL-based seamless transfer control between grid-connected and islanding modes in grid-connected inverters," *IEEE Trans. Power Electron.*, vol. 29, no. 10, pp. 5218–5228, Oct. 2014.

[104] G. G. Talapur, H. M. Suryawanshi, L. Xu, and A. B. Shitole, "A reliable microgrid with seamless transition between grid connected and islanded mode for residential community with enhanced power quality," *IEEE Trans. Ind. Appl.*, vol. 54, no. 5, pp. 5246–5255, Sep./Oct. 2018.

[105] X. Li, H. Zhang, M. B. Shadmand, and R. S. Balog, "Model predictive control of a voltage-source inverter with seamless transition between islanded and grid-connected operations," *IEEE Trans. Ind. Electron.*, vol. 64, no. 10, pp. 7906–7918, Oct. 2017.

[106] S. Yazdani, M. Ferdowsi, and P. Shamsi, "Internal model based smooth transition of a three-phase inverter between islanded and grid-connected modes," *IEEE Trans. Energy Convers.*, vol. 35, no. 1, pp. 405–415, Mar. 2020.

[107] M. Ganjian-Aboukheili, M. Shahabi, Q. Shafiee, and J. M. Guerrero, "Seamless transition of microgrids operation from grid-connected to islanded mode," *IEEE Trans. Smart Grid*, vol. 11, no. 3, pp. 2106–2114, May 2020.

[108] O. V. Kulkarni, S. Doolla, and B. G. Fernandes, "Mode transition control strategy for multiple inverter-based distributed generators operating in grid-connected and standalone mode," *IEEE Trans. Ind. Appl.*, vol. 53, no. 6, pp. 5927–5939, Nov. 2017.

[109] T. L. Vandoorn, B. Meersman, J. D. M. De Kooning, and L. Vandevelde, "Transition from islanded to grid-connected mode of microgrids with voltage-based droop control," *IEEE Trans. Power Syst.*, vol. 28, no. 3, pp. 2545–2553, Aug. 2013.

[110] S. D'silva, M. Shadmand, S. Bayhan, and H. Abu-Rub, "Towards grid of microgrids: Seamless transition between grid-connected and islanded modes of operation," *IEEE Open J. Ind. Electron. Soc.*, vol. 1, pp. 66–81, 2020.

[111] T. Qoria, F. Gruson, F. Colas, X. Kestelyn, and X. Guillaud, "Current limiting algorithms and transient stability analysis of grid-forming VSCs," *Electr. Power Syst. Res.*, vol. 189, Dec. 2020, Art. no. 106726.

[112] T. C. Green and M. Prodanovic, "Control of inverter-based micro-grids," *Electr. Power Syst. Res.*, vol. 77, no. 9, pp. 1204–1213, Jul. 2007.

[113] M. Brucoli, "Fault behaviour and fault detection in islanded inverter-only microgrids," Ph.D. dissertation, Dept. Elect. Electron. Eng., Imperial College London, London, U.K., 2008.

[114] C. A. Plet and T. C. Green, "A method of voltage limiting and distortion avoidance for islanded inverter-fed networks under fault," in *Proc. 14th Eur. Conf. Power Electron. Appl.*, 2011, pp. 1–8.

[115] K. O. Oureilidis and C. S. Demoulias, "A fault clearing method in converter-dominated microgrids with conventional protection means," *IEEE Trans. Power Electron.*, vol. 31, no. 6, pp. 4628–4640, Jun. 2016.

[116] K. Shi, W. Song, P. Xu, Z. Fang, and Y. Ji, "Low-voltage ride-through control strategy for a virtual synchronous generator based on smooth switching," *IEEE Access*, vol. 6, pp. 2703–2711, 2017.

[117] X. Lin, Y. Zheng, Z. Liang, and Y. Kang, "The suppression of voltage overshoot and oscillation during the fast recovery process from load short-circuit fault for three-phase stand-alone inverter," *IEEE Trans. Emerg. Sel. Topics Power Electron.*, vol. 9, no. 1, pp. 858–871, Feb. 2020.

[118] A. Gkountaras, S. Dieckerhoff, and T. Sezi, "Evaluation of current limiting methods for grid forming inverters in medium voltage microgrids," in *Proc. IEEE Energy Convers. Congr. Expo. (ECCE)*, Sep. 2015, pp. 1223–1230.

[119] L. Huang, H. Xin, Z. Wang, L. Zhang, K. Wu, and J. Hu, "Transient stability analysis and control design of droop-controlled voltage source converters considering current limitation," *IEEE Trans. Smart Grid*, vol. 10, no. 1, pp. 578–591, Jan. 2019.

[120] M. G. Taul, X. Wang, P. Davari, and F. Blaabjerg, "An overview of assessment methods for synchronization stability of grid-connected converters under severe symmetrical grid faults," *IEEE Trans. Power Electron.*, vol. 34, no. 10, pp. 9655–9670, Oct. 2019.

[121] M. Z. Mansour, S. P. Me, S. Hadavi, B. Badrazadeh, A. Karimi, and B. Bahrani, "Nonlinear transient stability analysis of phased-locked loop based grid-following voltage source converters using Lyapunov's direct method," *IEEE Trans. Emerg. Sel. Topics Power Electron.*, early access, Feb. 8, 2021, doi: 10.1109/JESTPE.2021.3057639.

[122] S. F. Zarei, H. Mokhtari, M. A. Ghasemi, and F. Blaabjerg, "Reinforcing fault ride through capability of grid forming voltage source converters using an enhanced voltage control scheme," *IEEE Trans. Power Del.*, vol. 34, no. 5, pp. 1827–1842, Oct. 2019.

[123] N. Bottrell and T. C. Green, "Comparison of current-limiting strategies during fault ride-through of inverters to prevent latch-up and wind-up," *IEEE Trans. Power Electron.*, vol. 29, no. 7, pp. 3786–3797, Jul. 2014.

[124] A. D. Paquette and D. M. Divan, "Virtual impedance current limiting for inverters in microgrids with synchronous generators," *IEEE Trans. Ind. Appl.*, vol. 51, no. 2, pp. 1630–1638, Mar./Apr. 2015.

[125] F. Welck, D. Duckwitz, and C. Gloeckler, "Influence of virtual impedance on short circuit performance of virtual synchronous machines in the 9-bus system," in *Proc. Conf. Sustain. Energy Supply Energy Storage Syst. (NEIS)*, 2017, pp. 1–7.

[126] G. Denis, T. Prevost, M. Debry, F. Xavier, X. Guillaud, and A. Menze, "The Migrate project: The challenges of operating a transmission grid with only inverter-based generation. A grid-forming control improvement with transient current-limiting control," *IET Renew. Power Gener.*, vol. 12, no. 5, pp. 523–529, Apr. 2018.

[127] X. Lu, J. Wang, J. Guerrero, and D. Zhao, "Virtual-impedance-based fault current limiters for inverter dominated AC microgrids," *IEEE Trans. Smart Grid*, vol. 9, no. 3, pp. 1599–1612, May 2018.

[128] Q.-C. Zhong and G. C. Konstantopoulos, "Current-limiting droop control of grid-connected inverters," *IEEE Trans. Ind. Electron.*, vol. 64, no. 7, pp. 5963–5973, Jul. 2017.

[129] J. Chen, F. Prystupczuk, and T. O'Donnell, "Use of voltage limits for current limitations in grid-forming converters," *CSEE J. Power Energy Syst.*, vol. 6, no. 2, pp. 259–269, 2020.

[130] I. Sadeghkhani, M. E. H. Golshan, J. M. Guerrero, and A. Mehrizi-Sani, "A current limiting strategy to improve fault ride-through of inverter interfaced autonomous microgrids," *IEEE Trans. Smart Grid*, vol. 8, no. 5, pp. 2138–2148, Sep. 2017.

[131] H. R. Baghaee, M. Mirsalim, G. B. Gharehpetian, and H. A. Talebi, "A new current limiting strategy and fault model to improve fault ride-through capability of inverter interfaced DERs in autonomous microgrids," *Sustain. Energy Technol. Assessments*, vol. 24, pp. 71–81, Dec. 2017.

[132] R. Rosso, S. Engelken, and M. Liserre, "Current limitation strategy for grid-forming converters under symmetrical and asymmetrical grid faults," in *Proc. IEEE Energy Convers. Congr. Expo. (ECCE)*, Oct. 2020, pp. 3746–3753.

[133] X. Lin, Z. Liang, Y. Zheng, Y. Lin, and Y. Kang, "A current limiting strategy with parallel virtual impedance for three-phase three-leg inverter under asymmetrical short-circuit fault to improve the controllable capability of fault currents," *IEEE Trans. Power Electron.*, vol. 34, no. 8, pp. 8138–8149, Aug. 2019.

[134] B. Mahamedi, M. Eskandari, J. E. Fletcher, and J. Zhu, "Sequence-based control strategy with current limiting for the fault ride-through of inverter-interfaced distributed generators," *IEEE Trans. Sustain. Energy*, vol. 11, no. 1, pp. 165–174, Jan. 2020.

[135] H. Wu and X. Wang, "A mode-adaptive power-angle control method for transient stability enhancement of virtual synchronous generators," *IEEE J. Emerg. Sel. Topics Power Electron.*, vol. 8, no. 2, pp. 1034–1049, Jun. 2020.

[136] T. Qoria, F. Gruson, F. Colas, G. Denis, T. Prevost, and X. Guillaud, "Critical clearing time determination and enhancement of grid-forming converters embedding virtual impedance as current limitation algorithm," *IEEE J. Emerg. Sel. Topics Power Electron.*, vol. 8, no. 2, pp. 1050–1061, Jun. 2020.

[137] J. Matevosyan, B. Badrzadeh, T. Prevost, E. Quitmann, D. Ramasubramanian, H. Urdal, S. Achilles, J. MacDowell, S. H. Huang, V. Vital, J. O'Sullivan, and R. Quint, "Grid-forming inverters: Are they the key for high renewable penetration?" *IEEE Power Energy Mag.*, vol. 17, no. 6, pp. 89–98, Nov./Dec. 2019.
[138] R. H. Lasseter, Z. Chen, and D. Pattabiraman, "Grid-forming inverters: A critical asset for the power grid," *IEEE J. Emerg. Sel. Topics Power Electron.*, vol. 8, no. 2, pp. 925–935, Jun. 2020.
[139] M. Ndreko, S. Rüberg, and W. Winter, "Grid forming control scheme for power systems with up to 100% power electronic interfaced generation: A case study on great Britain test system," *IET Renew. Power Gener.*, vol. 14, no. 8, pp. 1268–1281, Jun. 2020.
[140] B. K. Poolla, D. Groß, and F. Dörfler, "Placement and implementation of grid-forming and grid-following virtual inertia and fast frequency response," *IEEE Trans. Power Syst.*, vol. 34, no. 4, pp. 3035–3046, Jul. 2019.
[141] M. Raza, E. Prieto-Araujo, and O. Gomis-Bellmunt, "Small-signal stability analysis of offshore AC network having multiple VSC-HVDC systems," *IEEE Trans. Power Del.*, vol. 33, no. 2, pp. 830–839, Apr. 2018.
[142] M. Raza, M. A. Peñalba, and O. Gomis-Bellmunt, "Short circuit analysis of an offshore AC network having multiple grid forming VSC-HVDC links," *Int. J. Electr. Power Energy Syst.*, vol. 102, pp. 364–380, Nov. 2018.
[143] S. Tian, D. Campos-Gaona, V. A. Lacerda, R. E. Torres-Olguin, and O. Anaya-Lara, "Novel control approach for a hybrid grid-forming HVDC offshore transmission system," *Energies*, vol. 13, no. 7, p. 1681, Apr. 2020, doi: 10.3390/en13071681.
[144] S. Wang, J. Hu, X. Yuan, and L. Sun, "On inertial dynamics of virtual-synchronous-controlled DFIG-based wind turbines," *IEEE Trans. Energy Convers.*, vol. 30, no. 4, pp. 1691–1702, Dec. 2015.
[145] Y. Lei, W. He, M. Liao, B. Zang, J. Hu, and Y. Chi, "Inertia characteristics analysis of DFIG-based wind turbines with virtual synchronous control in different operation areas," in *Proc. IEEE Sustain. Power Energy Conf. (iSPEC)*, Nov. 2019, pp. 2238–2244.
[146] Y. Ma, W. Cao, L. F. Yang, F. Wang, and L. M. Tolbert, "Virtual synchronous generator control of full converter wind turbines with short-term energy storage," *IEEE Trans. Ind. Electron.*, vol. 64, no. 11, pp. 8821–8831, Nov. 2017.
[147] Y. Jiao and H. Nian, "Grid-forming control for DFIG based wind farms to enhance the stability of LCC-HVDC," *IEEE Access*, vol. 8, pp. 156752–156762, 2020.
[148] S. S. H. Yazdi, J. Milimonfared, S. H. Fathi, K. Rouzbehi, and E. Rakhshani, "Analytical modeling and inertia estimation of VSG-controlled type 4 WTGs: Power system frequency response investigation," *Int. J. Electr. Power Energy Syst.*, vol. 107, pp. 446–461, May 2019. [Online]. Available: http://www.sciencedirect.com/science/article/pii/S0142061518322191
[149] S. Sang, C. Zhang, X. Cai, M. Molinas, J. Zhang, and F. Rao, "Control of a type-IV wind turbine with the capability of robust grid-synchronization and inertial response for weak grid stable operation," *IEEE Access*, vol. 7, pp. 58553–58569, 2019.
[150] X. Quan, R. Yu, X. Zhao, Y. Lei, T. Chen, C. Li, and A. Q. Huang, "Photovoltaic synchronous generator: Architecture and control strategy for a grid-forming PV energy system," *IEEE J. Emerg. Sel. Topics Power Electron.*, vol. 8, no. 2, pp. 936–948, Jun. 2020.
[151] J. Liu, D. Yang, W. Yao, R. Fang, H. Zhao, and B. Wang, "PV-based virtual synchronous generator with variable inertia to enhance power system transient stability utilizing the energy storage system," *Protection Control Modern Power Syst.*, vol. 2, no. 1, pp. 1–8, Dec. 2017.
[152] A. Belila, Y. Amirat, M. Benbouzid, E. M. Berkouk, and G. Yao, "Virtual synchronous generators for voltage synchronization of a hybrid PV-diesel power system," *Int. J. Electr. Power Energy Syst.*, vol. 117, May 2020, Art. no. 105677. [Online]. Available: http://www.sciencedirect.com/science/article/pii/S0142061519302984
[153] S. Nogami, A. Yokoyama, T. Daibu, and Y. Hono, "Virtual synchronous generator model control of PV for improving transient stability and damping in a large-scale power system," *IEEJ Trans. Power Energy*, vol. 138, no. 8, pp. 716–723, 2018.
[154] A. Jain, J. N. Sakamuri, and N. A. Cutululis, "Grid-forming control strategies for black start by offshore wind power plants," *Wind Energy Sci.*, vol. 5, no. 4, pp. 1297–1313, Oct. 2020.
[155] A. Jain, O. Saborío-Romano, J. N. Sakamuri, and N. A. Cutululis, "Black-start from HVDC-connected offshore wind: Hard versus softenergization," *IET Renew. Power Gener.*, vol. 15, no. 1, pp. 127–138, 2021.
[156] A. W. Korai, E. Rakhshani, M. E. Adabi, J. L. R. Torres, and M. A. van der Meijden, "Modelling and simulation of wind turbines with grid forming direct voltage control and black-start capability," in *Modelling and Simulation of Power Electronic Converter Dominated Power Systems in PowerFactory*. Cham, Switzerland: Springer, 2020, pp. 245–268.
[157] S. Cherevatskiy, S. Sproul, S. Zabihi, R. Korte, H. Klingenberg, B. Buchholz, and A. Oudalov, "Grid forming energy storage system addresses challenges of grids with high penetration of renewables (a case study)," in *Proc. CIGRÉ Session*, vols. C2–C6, 2020, p. 322.
[158] S. Sproul, S. Cherevatskiy, and H. Klingenberg. (Jul. 2020). *Grid Forming Energy Storage: Provides Virtual Inertia, Interconnects Renewables and Unlocks Revenue*. Accessed: May 4, 2021. [Online]. Available: https://go.hitachi-powergrids.com/grid-forming-webinar-2020
[159] (2019). *Hornsdale Power Reserve: Year 2 Technical and Market Impact Case Study*. Aurecon. Accessed: May 4, 2021. [Online]. Available: https://hornsdalepowerreserve.com.au/wp-content/uploads/2020/07/Aurecon-Hornsdale-Power-Reserve-Impact-Study-year-2.pdf
[160] G. Parkinson. (Jul. 2020). *Tesla Big Battery at Hornsdale Delivers World Record Output of 150MW*. Renew Economy. Australia. Accessed: May 4, 2021. [Online]. Available: https://reneweconomy.com.au/tesla-big-battery-at-hornsdale-delivers-world-record-output-of-150mw-26392/
[161] E. Bellini. (Apr. 2020). *General Electric Works on Grid-Forming Inverter Controls*. PV Magazine International. Accessed: May 4, 2021. [Online]. Available: https://www.pv-magazine.com/2020/04/06/general-electric-works-on-grid-forming-inverter-controls/
[162] S. Djunisic. (Nov. 2020). *ScottishPower Completes Black Start Project Using 69-MW Wind Farm*. Renewables Now. Accessed: May 4, 2021. [Online]. Available: https://renewablesnow.com/news/scottishpower-completes-black-start-project-using-69-mw-wind-farm-719904/
[163] (2015). *Battery/Diesel Grid-Connected Microgrids: A Large-Scale, Industry-Based Case Study of Future Microgrid Capabilities*. ABB. Accessed: May 4, 2021. [Online]. Available: https://library.e.abb.com/public/0dd8532d75d14c49a6bc92cb91d71b30/Ausnet%20Services%20GESS%20white%20paper.pdf

DAYAN B. RATHNAYAKE (Student Member, IEEE) received the B.Sc. and M.Sc. degrees from the University of Peradeniya, Peradeniya, Sri Lanka, in 2014 and 2017, respectively, all in electrical and electronic engineering. He is currently pursuing the Ph.D. degree in electrical engineering with Monash University. His research interests include grid-forming inverters and control and stability analysis of inverter-based resources in low-inertia and weak grids.

MILAD AKRAMI received the B.Sc. and M.Sc. degrees in electrical engineering, focusing on power electronics from Sharif University of Technology, Tehran, Iran, in 2016 and 2019, respectively. He is currently pursuing the Ph.D. degree in power electronics with the University of Strasbourg, France. His current research interests include control of power electronic converters, electric vehicles, and sensorless drives.

CHITARANJAN PHURAILATPAM (Graduate Student Member, IEEE) received the bachelor's degree in electrical engineering from Malaviya National Institute of Technology, Jaipur, India, in 2010, the M.Sc.Eng. degree in energy and power systems from the University of Liverpool, U.K., in 2013, and the master's degree. He is currently pursuing the joint Ph.D. degree with the Indian Institute of Technology Bombay, India, and Monash University, Australia. He had worked as a Research Assistant at IIT Mandi, Himachal Pradesh, India. His current research interests include system integration and control of renewable/distributed energy sources for grid support applications and the security and stability of low-inertia systems.

SI PHU ME (Graduate Student Member, IEEE) received the B.E. degree in electrical and computer systems engineering from Monash University, Victoria, Australia, in 2019, where he is currently pursuing the Ph.D. degree in power electronic engineering.

His research interests include the control and stability analysis of power converters.

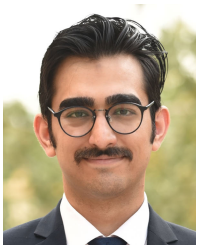

SAJJAD HADAVI (Student Member, IEEE) received the B.Sc. and M.Sc. degrees in electrical engineering from Amirkabir University of Technology, Tehran, Iran, in 2013 and 2015, respectively. He is currently pursuing the Ph.D. degree with Monash University, Australia. His research interests include control of power electronics systems, power electronics in power systems, and grid integration of renewable energy resources.

GAMINI JAYASINGHE (Senior Member, IEEE) received the B.Sc. degree in electronic and telecommunication engineering from the University of Moratuwa, Sri Lanka, in 2003, and the Ph.D. degree in electrical engineering from Nanyang Technological University, Singapore, in 2013. From 2011 to 2015, he worked as an Electrical Systems Engineer at the Rolls Royce Advanced Technology Centre, Singapore. From 2015 to 2021, he worked as a Senior Lecturer in maritime electrical engineering with the Australian Maritime College, University of Tasmania, Launceston, Australia. He is currently working as a Research Fellow with the Department of Electrical and Computer Systems Engineering, Faculty of Engineering, Monash University, Australia. His research interests include power electronic converters, renewable energy technologies, grid integration of energy systems, shipboard power systems, and electric vehicles and control systems.

SASAN ZABIHI (Senior Member, IEEE) received the Ph.D. degree in power electronics control and applications from Queensland University of Technology (QUT), Australia, in 2011. He then served as a Lecturer at QUT, until 2012. Prior to joining QUT in 2008, he was a Senior Development Engineer with multiple energy research institutes, focusing on control and topology design for power conversion and custom power devices. Since 2013, he has been a Research and Development Specialist with ABB Australia (now HITACHI ABB Power Grids), in their global CoC for micro-grid, and distributed generation, developing power converters, and associated control for microgrids, energy storage, and Renewable applications, and facilitating their integration into power systems. His focus lately has been shifted to addressing transient stability and system strength challenges ahead of our future grids with the ever-increasing penetration of renewables. He is currently an Adjunct Associate Professor at Monash University. He is an Active Member of several CIGRE working groups and IEEE task forces.

BEHROOZ BAHRANI (Senior Member, IEEE) received the B.Sc. degree from Sharif University of Technology, Tehran, Iran, the M.Sc. degree from the University of Toronto, Toronto, ON, Canada, and the Ph.D. degree from the Ecole Polytechnique Federale de Lausanne (EPFL), Lausanne, Switzerland, all in electrical engineering, in 2006, 2008, and 2012, respectively. From September 2012 to September 2015, he was a Postdoctoral Fellow at EPFL, Purdue University, West Lafayette, IN, USA; Georgia Institute of Technology, Atlanta, GA, USA; and the Technical University of Munich, Munich, Germany. Since 2015, he has been with Monash University, where he is currently a Senior Lecturer and the Director of the Grid Innovation Hub. His research interests include control of power electronic converters, their applications in power systems, and grid integration of renewable energy resources.